Turkish Journal of Earth Sciences

Volume 32 | Number 4 Article 7

1-1-2023

Micropaleontological findings and absolute ages mark the termination of the Last Glacial Maximum in the Eastern Mediterranean Region: New electron spin resonance data from Gediz Delta (Western Turkey)

EKİN GÖKÇE BENLİ

HÜLYA ASLIN

İSMAİL İŞİNTEK

BİROL ENGİN

BERNA ŞENGÖÇMEN GEÇKİN

Follow this and additional works at: https://journals.tubitak.gov.tr/earth

 Part of the Earth Sciences Commons

Recommended Citation

BENLİ, EKİN GÖKÇE; ASLIN, HÜLYA; İŞİNTEK, İSMAİL; ENGİN, BİROL; and GEÇKİN, BERNA ŞENGÖÇMEN (2023) "Micropaleontological findings and absolute ages mark the termination of the Last Glacial Maximum in the Eastern Mediterranean Region: New electron spin resonance data from Gediz Delta (Western Turkey)," *Turkish Journal of Earth Sciences*: Vol. 32: No. 4, Article 7. https://doi.org/10.55730/1300-0985.1859

Available at: https://journals.tubitak.gov.tr/earth/vol32/iss4/7

This Article is brought to you for free and open access by TÜBİTAK Academic Journals. It has been accepted for inclusion in Turkish Journal of Earth Sciences by an authorized editor of TÜBİTAK Academic Journals. For more information, please contact academic.publications@tubitak.gov.tr.

TÜBİTAK

Turkish Journal of Earth Sciences

http://journals.tubitak.gov.tr/earth/

Research Article

Turkish J Earth Sci
(2023) 32: 520-540
© TÜBİTAK
doi:10.55730/1300-0985.1859

Micropaleontological findings and absolute ages mark the termination of the Last Glacial Maximum in the Eastern Mediterranean Region: New electron spin resonance data from Gediz Delta (Western Turkey)

Ekin Gökçe BENLİ[1,*], Hülya ASLIN[2], İsmail İŞİNTEK[3], Birol ENGİN[4], Berna ŞENGÖÇMEN-GEÇKİN[5]

[1]Department of Geological Engineering, Faculty of Engineering, Kocaeli University, İzmit, Kocaeli, Turkey
[2]Esentepe mah. Ergene vadisi sitesi C6/23 Çorlu, Tekirdağ, Turkey
[3]Department of Geological Engineering, Faculty of Engineering, Dokuz Eylül University, İzmir, Turkey
[4]İzmir Metropolitan Municipality-İzenerji-Su Kaynakları Araştırma ve Uygulama Birimi, İzmir, Turkey

Received: 07.07.2022 • **Accepted/Published Online:** 11.04.2023 • **Final Version:** 29.05.2023

Abstract: Sediments and fossil content of Gediz Delta (Eastern Aegean Sea-*İzmir) were examined from the samples collected from three drilling cores from* the west (seaward) to east (landward) of the delta. Each drilling core contains-Quarternary marine deposits with a marine fauna of foraminifers, bivalves, gastropods, echinoids, and ostracods at the bottom and Quaternary continental delta deposits at the top. According to our Electron Spin Resonance (ESR) age model marine sediments of the Aegean Sea started to cover the western Gediz Delta area before 19.9 ka (thousand years). Following the Last Glacial Maximum (LGM), after the transgression due to deglaciation occurred 15.3 ka ago, the coastline progressed 15–20 km eastward and covered the entire delta area. At the end of the LGM, as a result of the overflow of Manisa Gediz Lake depending on the deglaciation in Western Anatolia, and its flow from the Emiralem Strait to the İzmir Bay, the continental deposits reaching the West Gediz Delta region are younger than 11.4 ka.

Key words: Gediz Delta, recent foraminifers, Holocene, late Pleistocene, electron spin resonance, Last Glacial Maximum

1. Introduction

The Last Glacial Maximum (LGM) represents the most recent time during which ice sheets were most widespread during the Last Glacial Period (LGP) (Steven, 2004). At this time, ice sheets covered much of northern North America, northern Europe, and Asia, causing a massive drop in sea levels, profoundly affecting Earth's climate (Steven, 2004). In multiple recent studies in many parts of the world, the growth of ice sheets began 33 ka ago and the maximum coverage was between 26.5 ka and 19–20 ka in the Northern Hemisphere. The decline of the ice sheet occurred approximately 14.5 ago (Clark et al., 2009, Evans et al., 2014). The places where the effects of glacial periods are best observed around the coastal belts, deltas, and inland seas such as the Marmara Sea (Smith et al., 1995; Çağatay et al., 2000; Aksu et al., 2002) and the Black Sea (Lericolais et al., 2008; Aksu et al., 2022) where sea level falls or rises leaving the best traces. Smith et al. (1995), stated that 13 ka ago, with the onset of deglaciation, the Sea of Marmara was filled with Mediterranean waters. Çağatay et al. (2000) expressed that the late Quaternary sediments of the Marmara Sea basin were deposited in a freshwater lake during the LGM ca to 12 ka ago. Aksu et al. (2002) emphasized that the Marmara Sea basin, which was a freshwater lake during the LGM, turned into fully marine conditions with the flow of Mediterranean waters ca 11–10.5 ka ago. In addition, Lericolais et al., 2008, mention lowstand period deposits between the last 11 ka and 8.5 ka (^{14}C age) and a drape of marine mud that suddenly covers all the lowstand deposits. In these mentioned studies carried out in the Eastern Mediterranean Sea, the Sea of Marmara, and the Black Sea, there is a consensus that the sea levels during the LGM were 80–100 m lower than the current sea level. In this context, The Gediz Delta is one of the best places where the latest LGM effects can be observed and some studies (Aksu and Piper, 1983, 1984; Aksu et al., 1995; Hakyemez et al., 1999, 2013) were carried out in the Eastern Mediterranean Region. The Gediz Delta, which is a remarkable late Quarternary geologic and geographic formation of western Anatolia, lies on the northeast side of İzmir Bay and covers a large area between Karşıyaka, Menemen, and Foça districts (Figure 1). Scientific records on the delta date back to the 1800s. In the oldest records, the Gediz River and its delta were named as "Hermus

* Correspondence: ekinbenli13@gmail.com

This work is licensed under a Creative Commons Attribution 4.0 International License.

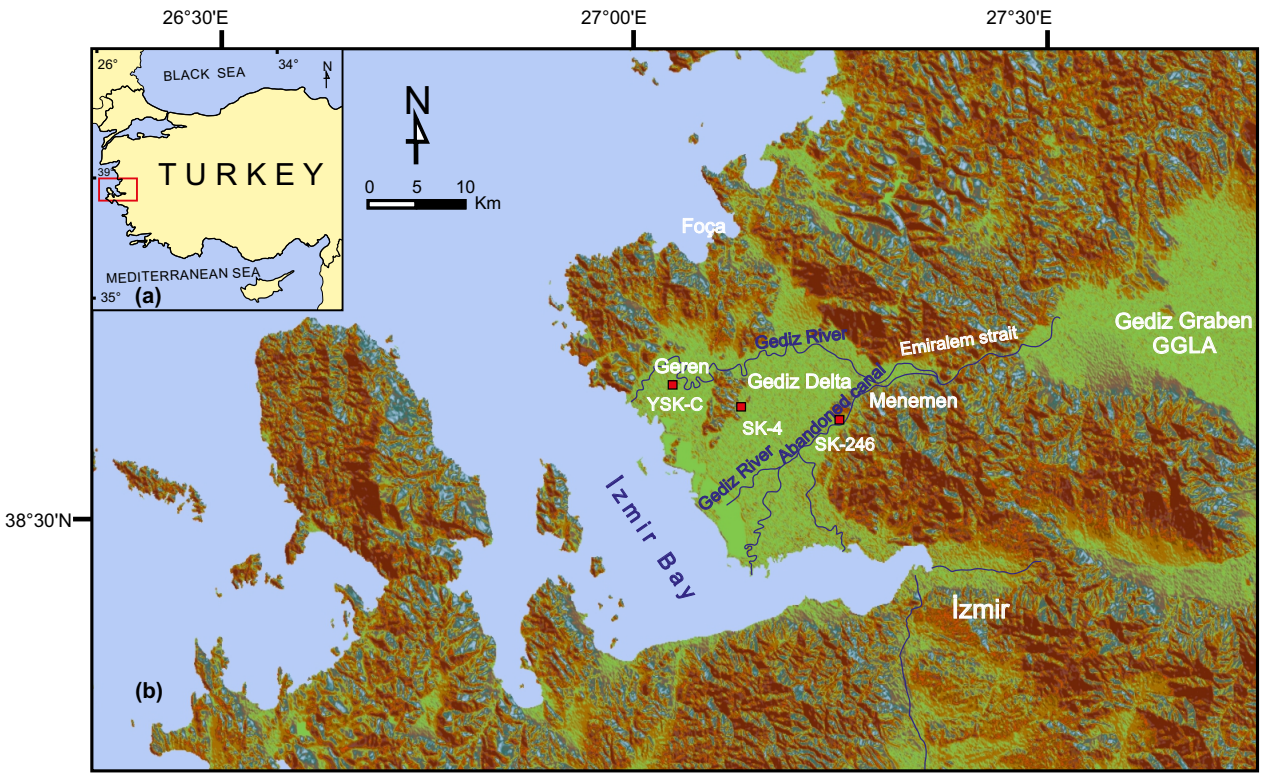


Figure 1. a) Location of Gediz delta in Türkiye, b) Topographic Map of Gediz Delta and surrounding region and location of drilling cores. Topographic data were obtained by a Digital Elevation Model (DEM) image with ~127 m ground resolution. This figure was prepared using Arcmap. GGLA: Gediz Graben Lake Area of the Hakyemez et al., 1999, 2013.

River" and "Delta of the Hermus", respectively, Strabon (7 BC) (Jones, 1917), Herodotus (430 BC) (Godley, 1920), and Strickland (1937). However, Spratt (1845) used the names "Ancient Hermes" and "Kedooz Tchai" for the Gediz River. According to Ottoman records, in the early 19th century, the sediments of the Gediz River began to fill the Gulf of İzmir. Therefore, the main channel of the river was changed by the cooperation of Germans and Ottomans (Ottoman Archive, 1887, 1889). In the second half of the 21st century, the geology of the delta and its periphery have been studied in more detail (Şenel, 2002; Kayan and Öner, 2015).

In more recent and detailed geological studies (Aksu and Piper, 1983, 1984) based on seismic and archeologic data, it is mentioned that during the LGM, the current Gediz Delta area is at the lowest sea level (about 120 m), and the Aegean Sea shoreline located off the coast of Foça. Aksu and Piper (1983, 1984) suggested that until the end of the LGM (16 ka before present -BP-), from Foça to Menemen was under continental conditions. These authors emphasize that the continental delta sediments start to fill the delta area at around 3 ka BP. Thus, they have pointed out that the marine regression has been continuing since 3 ka. The results and comments of these authors are parallel to Fleming et al. (1998)'s data on eustatic sea level changes since the LGM. It can be inferred that the LGM, affecting the Gediz Delta, accepted in different intervals ranging from 30 ka to 13 ka BP in the Mediterranean province (Fairbanks, 1989; Stirling et al., 1995; Dias et al., 2000; Lambeck et al., 2002, Aksu et al., 2002; Lambeck and Purcell, 2005; Ergin et al., 2007, Kazancı, 2009; Milker et al., 2011). Post-LGM, instead, was marked with sea surface temperatures 5 to 10 °C warmer between 14 ka and 9.6 ka BP, as revealed by Aksu et al. (1995) based on their paleoclimatic, micropaleontological and stochastic isotope (^{18}O).

More recently, Hakyemez et al. (1999, 2013) have suggested that from the end of the LGM (16 ka BP) to the Early Holocene (11.7 ka–8.2 ka BP), sea-level gradually raised and probably in the Early Holocene reached its maximum level. According to these authors, in the Middle Holocene interval, as a result of the back erosion of the ancient Gediz River, the Gediz Delta area was connected to Plio-Quarternary Gediz Graben Lake for the first time. The same authors suggested that the continental sediments of the Gediz Delta were deposited during the Middle Holocene (approximately 7 ka) when the Gediz River crossed the Emiralem Strait and started to flow into the

İzmir Gulf (Figure 1). Since then, the waters of the Gediz Graben Lake discharge through the Gediz Delta (Figure 1). This reflects the fact that the regressive sediments of the Gediz Delta have been deposited since the end of the Early Pleistocene (11.7 ka–8.2 ka) (Hakyemez et al. 1999 and 2013). On the other side, according to the most recent geological studies, it is emphasized that the Gulf of İzmir and its surrounding are represented by the deposits of two superimposed Miocene and Plio-Quaternary basins (Uzel et al., 2008, 2012). In these studies, the authors described the main Gediz Delta deposits as part of the younger Plio-Quaternary tectonosedimentary basin, which is formed under the control of tectonic events. Although many researchers have studied the geological evolution of the Gediz Delta in terms of progradation and retrogradation of the delta shoreline based on sedimentological, geophysical, paleontological, and archaeological methods (Aksu and Piper, 1983, 1984; Hakyemez et al. (1999, 2013); Kayan and Öner, 2015), absolute dating of these sedimentary units has never been attempted. However, the presence and distribution of marine fossils are very concrete evidence for sea movements and the ESR (Electron Spin Resonance) method is a reliable absolute dating method that is applied frequently to fossil shells (Ikeya and Ohmura, 1981; Engin et al., 2006; Skinner and Shawl, 1994). Thus, this study aimed to reexamine the environmental, sedimentologic evolution, macro and micro faunal characteristics of the delta deposits developed across the LGM and obtain new absolute age data by using the ESR method.

2. Geological setting

The Gediz Delta deposits take place on a basement that consists of the Late Cretaceous-Paleocene Bornova Flysch Zone (Okay and Siyako, 1993) and Neogene volcanosedimentary succession (Figures 1, 2, 3).

The Bornova Flysch Zone, with a tectonic contact on the Menderes Massif in the region (Erdoğan, 1990), contains the latest Cretaceous-Paleocene deep marine sandstone-shale deposits (Erdoğan, 1990; Okay and Siyako, 1993; Sarı, 2014), and a mixture of fossiliferous and biolastic limestone block of Triassic to Cretaceous carbonate, mafic-ultramafic rocks of unknown age and chert mega-blocks of Jurassic to late Cretaceous age (Erdoğan, 1990; Okay and Altuner, 2007; Tekin and Göncüoğlu, 2007, 2009; Tekin et al., 2012). The rocks of the Menderes Massif are represented by mica schists and marbles in the close vicinity of the Gediz Delta (Erdoğan, 1990). The Neogene volcanosedimentary succession unconformably

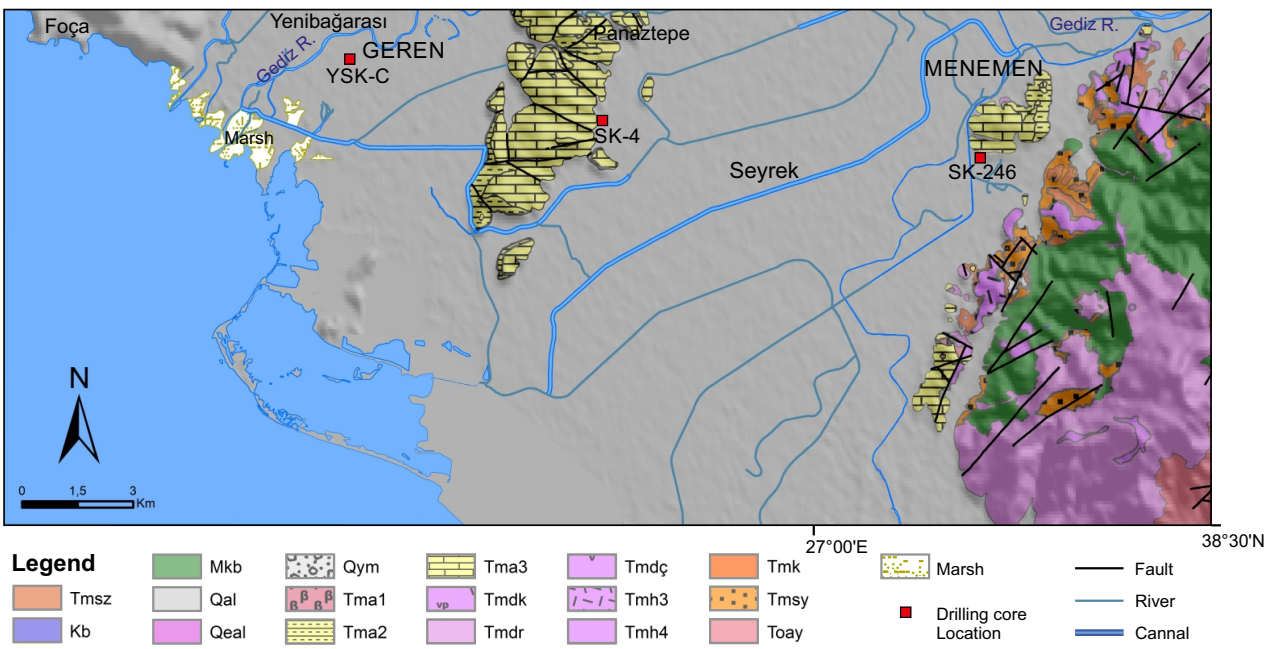


Figure 2. Generalized geological map of the Gediz Delta and surrounding region (Modified from Dönmez, 1992); Q Alluvial deposit; Tma_3 Yellow-white colored, locally siliceous lacustrine limestone, claystone-clayey limestone intercalation; Tma2 Light green, tuff-tuffite and pyroclastics; Tmd Dumanlıdağ volcanites (Dumanlıdağ Group); Tmdç Çukurköy volcanite grey coloured with coarse phenocryst andesite; Tmdr Rahmanlar agglomerate, basalt, andesite, pyroxene andesite, basaltic pebble and agglomerate with blocks, tuff; Tmh_4 Hasanlar volcanites basaltic agglomerate, tuff, lava; Tmh_3 Hasanlar volcanites black-brown coloured basalt; Tmsz Zeytindağ formation thin coal-bearing intervals, sandstone, claystone, clayish limestone, limestone intercalation; Tmsy Yeniköy weighted pebbly blocky alluvial fan deposit; Mkb in Bornova complex, flyshmatrix unit containing various rocks blocks.

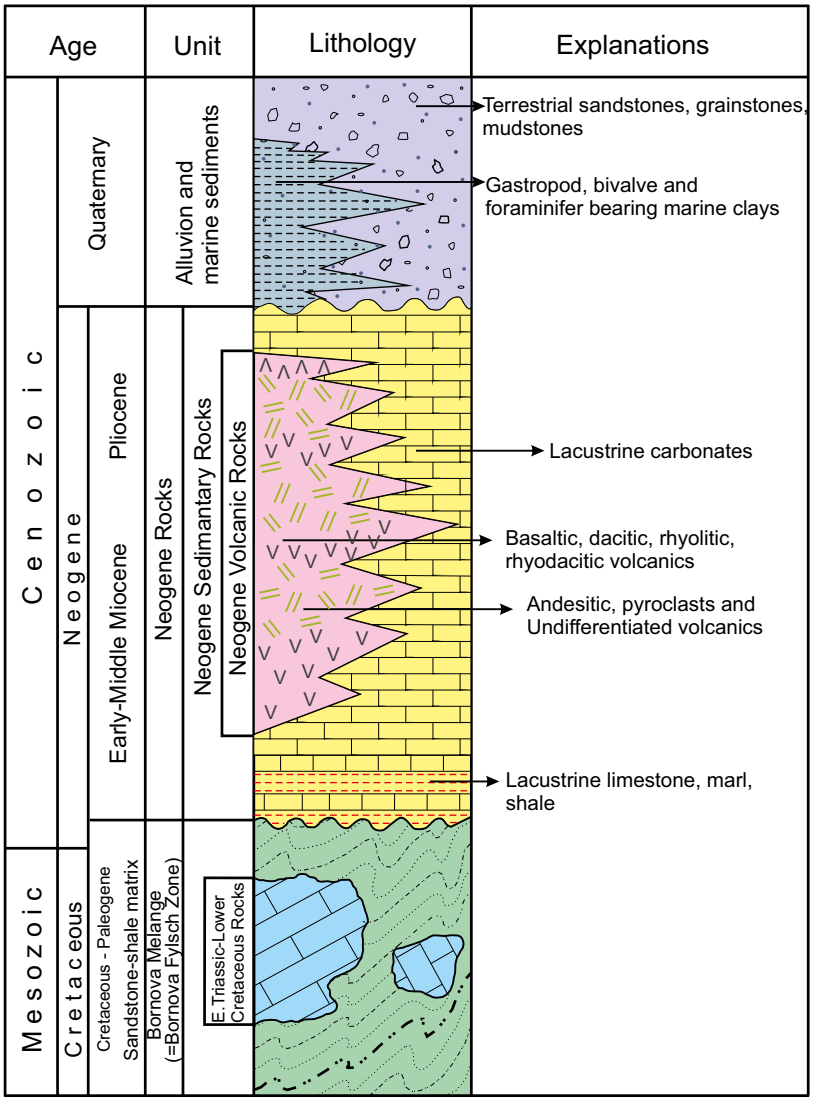


Figure 3. Generalized lithostratigrafic columnar section of İzmir and the surrounding area (after MTA, (2002) 1/1,500,000 scale geology map of Turkey, Hakyemez et al., 2013 and Uzel et al., 2008).

covers the Bornova Melange and is represented by brackish or freshwater lacustrine sediments and terrestrial clastics intercalated with andesitic, rhyolitic volcanic rocks (Erdoğan, 1990; Türkecan et al., 1998; Akay, 2001, 2004; Kaya et al., 2004; Emre et al., 2006b; Helvacı et al., 2009; Göktaş, 2014; Seghedi et al., 2015). Lacustrine sediments are moderately petrified and sparsely fractured and consist of whitish-yellow mudstone, limy claystone, clayey limestone, and limestone. Terrestrial sediments are laterally and vertically inter-fingered with lacustrine deposits and contain muddy conglomerate, mudstone, pebbly mudstone, and limy mudstone. The Neogene volcanic rocks intercalating with Neogene sediments are represented by andesitic, rhyolitic massive lavas, tuffs, and agglomerates (Türkecan et al., 1998; Akay, 2001, 2004).

Uzel et al., (2012) suggested that the Neogene sequence divided into Early-Middle Miocene "older basin fill" and Middle-Late Miocene "younger basin fill" separated from each other along an unconformity surface. The "older basin fill" consists of terrestrial and lacustrine sediments at the bottom and andesitic Yamanlar Volcanics at the top. The "younger basin fill" is represented by terrestrial and lacustrine deposits and contains massive basaltic lavas (Beşyol basalt) and is covered by rhyolitic lavas (Cumaovası volcanics).

In previous studies, the Gediz Delta sediment fill has generally been described as Holocene alluvial fan, delta sediments, and stream sediments (Hakyemez et al., 1999; Hakyemez et al., 2013). In some studies, they are shown as

Holocene alluvial fan and fan delta deposits interlaced with shallow marine sediments (Uzel et al., 2012). However, due to insufficient subsurface data, the thickness, geometry, and lithofacies of those marine sediments could not be documented in detail (Uzel et al., 2012). In some previous studies, based on submarine cores, seismic data, and archaeological evaluations (Plinius (23AD)), (Rackham, 1967), it is argued that the delta is represented by shallow marine sediments from 10 ka to 3 ka ago and by terrestrial delta sediments from 3 ka to the present (Aksu and Piper, 1983, 1984; Aksu et al., 1990; Aksu et al., 1995).

By general agreement, the delta area was filled with marine sediments by the effect of marine transgression, from the latest Pleistocene to Middle-Late Holocene time after the end of the LGM (Aksu and Piper, 1983, 1984 and Hakyemez et al., 2013). In the Middle or early Late Holocene period, with the Gediz River and Gediz Lake waters (Hakyemez et al., 2013) starting to flow into İzmir Gulf, the Delta area is filled with regressive continental delta deposits and is still being filled (Aksu and Piper, 1983, 1984; Hakyemez et al., 2013).

3. Material and methods

3.1. Drilling cores

In this study, three drilling cores from YSK-C, SK-4, and SK-246 boreholes were used to reveal the stratigraphy of delta deposits consisting of marine and terrestrial facies. The investigated drillings are approximately 3.9 (YSK-C), 9.4 (SK-4), and 19.4 (SK-246) km from the coastline in the E-W direction with elevations of 3 (Geren), 5 (Seyrek), and 6 (Menemen) m above sea level, respectively (Figures 1 and 2). The stratigraphy of these drilling cores is described in detail in section 4.1. Three drilling cores representing the seaside (from Geren location, total core thickness: 35 m), central part (from Seyrek Village, total core thickness: 15 m), and inland (from Menemen district, total core thickness: 45 m) of the Gediz Delta were examined in this study. The YSK-C drilling is located on the southwest of the Geren village, in the westernmost part of the Gediz Delta (Figures 1 and 2). The SK-4 core is located in the northwest of Seyrek (Menemen) village, in the western part of the Gediz Delta (Figures 1 and 2). The SK-246 drilling is located on the western edge of the Menemen district, where the delta plain begins (Figures 1 and 2).

3.2. Micropaleontological methods

The marine fossil-rich parts with a high core percentage were sampled in 1 m intervals. Either all or half of the sediments obtained from cores were processed. No sampling was made from the core gaps. Selected wet sediment samples were treated with 10% H_2O_2 solution for 24 h. Each sample was washed with pressurized water through 0.063 and 0.425 mm sieves and dried at 40 °C in the oven. Foraminifera, gastropods, bivalves, ostracods, echinoids, and worm tube individuals were separated under a binocular microscope. The foraminiferal descriptions and nomenclature used here are based on Cimerman and Langer (1991); Sgarrella and Moncharmont-Zei (1993); Hottinger et al. (1993); Loeblich and Tappan (1988); Avşar and Meriç (2001); Avşar and Ergin (2001); Meriç and Avşar (2001); Avşar (2002, 2008); Kaminski et al. (2002); Meriç et al. (2002; 2004a, 2004b, 2014; 2005); Avşar et al. (2006); Murray (2006).

3.3. The ESR dating method and measures

Age determination of 3 samples was carried out by applying ESR spectroscopic method. This method is based on measurements of the number of paramagnetic centers produced by natural radiation in geological material. The lattice of the biogenic shell carbonate does not have these centres at the time of its formation, but the ionizing radiation from the shell itself and the surrounding environment (enclosing matrix and cosmic ray) causes the gradual generation and subsequent accumulation of paramagnetic centres during its burial in the sediments (Molodkov, 2020). The number of these long-lived (about 10^6 to 10^9 years) centres is directly related to the total radiation dose that the shell has received, and, therefore, to the age of the shell and of the enclosing sediments (Molodkov, 2020). Details of the physical basis of ESR dating can be found elsewhere (Grün, 1989; Ikeya, 1993; Rink, 1997; Ulusoy et al., 2014; Blackwell et al., 2016). For the ESR dating method, according to fauna density, marine fossil shells such as bivalve, gastropod, echinoid, and ostracod were obtained from different ranges (8.00–9.00 m, 24.00–25.00 m, 25.00–26.00 m) of the core, YSK-C (Figure 4). These carbonate fossil shell samples for the ESR measurements were granulated by applying a light force in a porcelain mortar. After that, granulated shell material was sieved, and the 100–200 μm portion was separated for use. In the next step, the sieved samples were washed with 0.5% acetic acid (CH_3COOH) solution for about one min, then rinsed with distilled water to remove surface defect ESR signal at g = 2.0002 caused by α rays or applied external mechanical force (Engin et al., 2006; Aydaş et al., 2015). Finally, samples were dried in an oven at 40 °C.

These steps were repeated for each fossil sample taken from intervals of (8.00–9.00 m), (24.00–25.00 m), and (25.00–26.00 m) of YSK-C drilling core. In all ESR experimental procedures for the determination of the geological age above mentioned fossil shells, these powder-prepared samples were used. After the sample preparation procedure, each fossil sample was divided into several aliquots. After that, they were irradiated by calibrated gamma radiation doses and analyzed at room temperature by a Bruker e-scan X-band spectrometer. Comparable results were also obtained with a Bruker EMX 131 X-band ESR spectrometer. In this work, the combining ESR signal intensity at g = 2.0012 of the CO_2- paramagnetic ions was used as a dating signal which is indicated by the

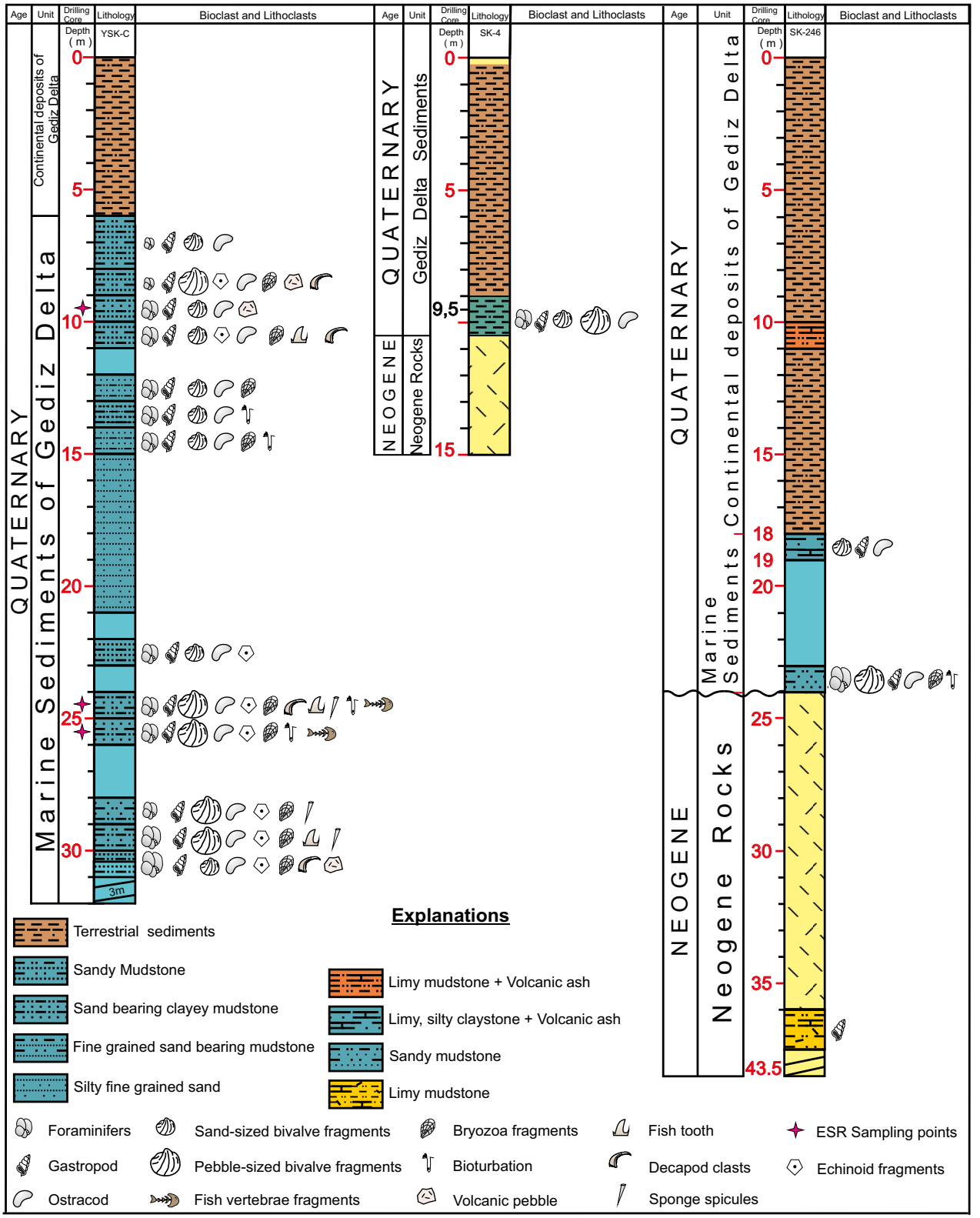


Figure 4. Lithological log and fossil contents of YSK-C, SK-4 and SK-246 drilling cores.

arrow in Figure 5(a). The radiation-induced paramagnetic centre concentration was obtained from the peak-to-peak amplitude of the g = 2.0012 ESR signal. Equivalent doses representing the accumulated natural radiation doses (AD) were obtained by employing the multiple-aliquot additive dose method (Ikeya, 1993; Küçükuysal et al., 2011; Aydaş et al., 2015). AD values were obtained by extrapolating the dose-response curves to zero ESR intensities. Dose-response curves were best fitted to the single saturation exponential function for the samples taken from 8.00–9.00 m and to the linear function for the other two. Curve fitting and statistical analysis were done with the software Origin 6.0. ESR spectrum and fitted dose-response curve of the samples taken from the depth of 8–9 m, are shown in Figure 5(b), respectively. The AD values of the fossil shell samples collected from depths of 8.00–9.00 m, 24.00–25.00 m, and 25.00–26.00 m were obtained as 34.6 ± 1.7, 53.5 ± 2.6, and 63.4 ± 3.1 Gy, respectively. Annual dose rates were determined, using the natural radioactive element (^{238}U, ^{232}Th, ^{40}K) concentrations, cosmic dose rate contribution, grain sizes of powders, and moisture effect. The annual dose rates for the three shell samples taken from 8.00–9.00, 24.00–25.00, and 25.00–26.00 m depths were calculated as 3.03, 3.49, and 3.17 mGy/a, respectively. ESR ages of fossil shell samples were estimated by taking into account the uranium uptake history of shells using the ROSY program (Brennan et al., 1997; Brennan et al., 1999).

In the study, the thermal behavior and structure of gastropod and bivalve shell samples were investigated by using Fourier Transform Infrared Spectroscopy (FTIR), X-ray Diffraction (XRD), ESR Spectroscopy and Thermal Gravimetric Analysis (TGA) techniques. ESR measurements were carried out at Dokuz Eylül University Faculty of Science, Department of Physics. The linear uptake (LU) method (Ikeya, 1993; Brennan et al., 1997; Brennan et al., 1999) is accepted as the calculation method.

4. Results

4.1. Stratigraphical results of the drilling cores

4.1.1. Stratigraphy of YSK-C core

The YSK-C drilling core (Figures 1, 2, and 4), from base to top, consists of shallow marine at 35.00–6.00 m below and terrestrial sediments from 6.00 m upwards. The marine section starts with sandy mudstone at the bottom and continues with rare sand-bearing mudstone. The middle part (22.00–15.00 m) is represented by silty fine sand layers (Figure 4). The upper part (15.00–6.00 m) is represented by thin mudstone and sandy mudstone. In the lower part of the core (31.00–22.00 m), a mudstone level includes abundant 1–4 mm in size gastropod, echinoid, bivalve, worm tube fragments, and an abundant amount of foraminifer and ostracod. At the base of the core (30.00–29.00 and 25.00–24.00 m), the common fossil is a bivalve, which still lives in abundance in the İzmir Bay (Figure 4).

The lower part of the core (31.00–30.00 m) includes abundant mica sands and more rarely volcanic pebbles. The terrestrial top section corresponding to 6.00–0.00 m of the YSK-C borehole has not been examined in detail in this work. However, this continental level is composed of unconsolidated muddy pebble stones, which also contain soil, and pebbly sandy mudstones, including the current deposits at the upper part of the Gediz Delta (Akçığ et al., 2012) (Figure 4).

4.1.2. Stratigraphy of SK-4 core

The 15 m long core is represented by an organic soil of 0.25 m at the top, terrestrial fragments up to 8.00 m below

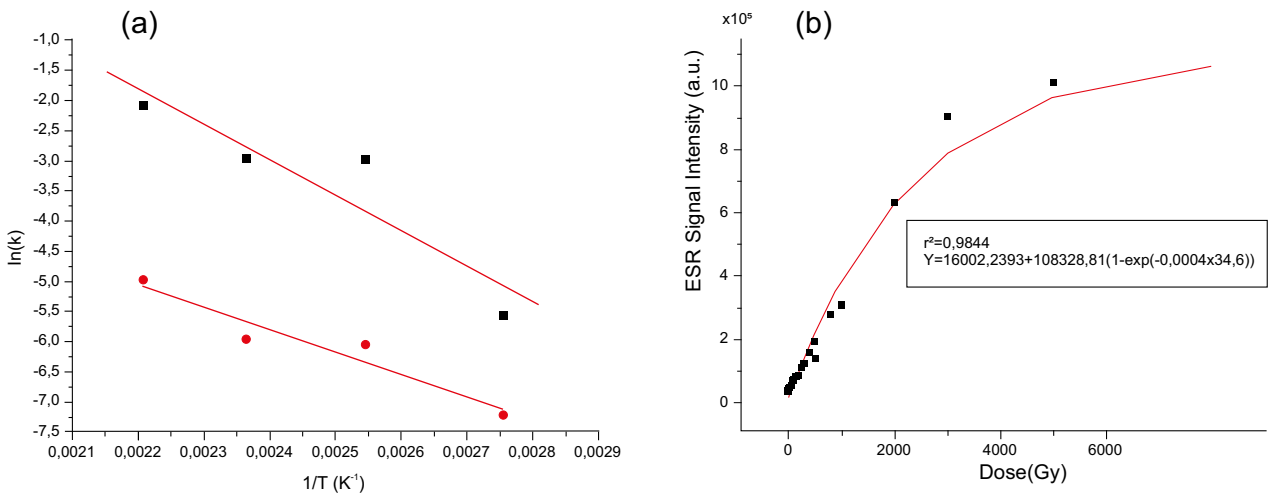


Figure 5. (a) ESR spectrum of 8 kGy irradiated fossil shells taken from 8.00–9.00 m depth (b) Dose-response curve of CO_2- signal (g = 2.0012) observed in mollusc shells.

it, marine sediments between 8.00–10.50 m, and Neogene volcanoclastic rocks at the bottom. The marine level (15.00–10.50 m) in the middle part consists of sandy, limy mudstone and contains abundant bivalves, gastropods, ostracods, and foraminifers (Figure 4). The contact between the Neogene clastics and the marine layers is a stratigraphic unconformity.

4.1.3. Stratigraphy of SK-246 core

The SK-246 drilling represents the E-NE boundary of the Gediz Delta. The 45 m core of SK-246 includes terrestrial Neogene layers at 45.00–24.00 m in the bottom, two marine levels at 24.00–23.00 m, and 19.00–18.00 m in the middle part. The rest of the core sequence is entirely represented by continental sediments (Figure 4).

The lower marine beds (24.00–23.00 m) are composed of sandy mudstones and contain abundant gastropods, foraminifers, echinoid fragments, worm tubes, bryozoa, and bivalves. Last, the upper marine beds (19.00–18.00 m) are represented by silt-bearing clayey limestone or lime claystone containing 0.5–5 mm in size ostracods, gastropods, and bivalve fragments and reworked volcanic ash. The upper marine layers do not include foraminifers. The rest of the sequence is represented by limy claystone and limy mudstone containing abundant lapilli size volcanic fragments. There are no marine fauna remains in this part (Figure 4). These deposits consist of probably reworked material of Neogene pyroclastic levels.

4.2. Micropaleontological results

4.2.1. Fossil content of the Gediz Delta in YSK-C, SK-246, and SK-4 cores

In this study, 66 foraminiferal species belonging to 41 genera were identified in samples collected from YSK-C, SK-246, and SK-4 drilling cores (Figures 1, 2). Within this assemblage, four species of *Haynesina germanica* (Ehrenberg), *Nonionella turgida* (Williamson), *Ammonia compacta* (Hofler), and *Elphidium crispum* (Linnaeus) are commonly found. Only two genera are planktonic and the rest is benthic foraminifers. In addition, samples include abundant bivalves, gastropods, and worm tubes. Along with the foraminifer assemblage, echinoid, bryozoa, sponge, decapod fragments and fish bones (tooth and vertebrae) are also abundant (Figures 6, 7, and 8).

4.2.2. Fosil content of the YSK-C core

In the YSK-C core, from bottom to top, 13 samples from different intervals were examined. Each sample is rich in bivalve, gastropod, and ostracod fragments (especially at 10.00–9.00 m) and foraminifer (Figures 4, 9). Observed bivalves in 9.00–8.00; 26.00–24.00, and 30.00–28.00 m are 2–60 mm in size. In the YSK-C core, 62 foraminifera species belonging to 38 genera were determined (Figures 6, 10, 11). Foraminifers in the range of 6.00–14.00 m are *Lagenammina* cf. *Laguncula* Rhumbler, *Hyperammina friabilis* Brady, *Hyperammina* sp., *Textularia bocki* Höglund, *Miliolinella subrotunda* (Montagu), *Pseudotriloculina* cf. *rotunda* (d'Orbigny), *P. subgranulata* (Cushman), *Wellmanellinella striata* (Sidebottom), *Valvulineria bradyana* (Fornasini), *Ammonia beccarii* (Linnaeus), *A. parkinsoniana* (d'Orbigny), *Ammonia compacta* (Hofler), *Porosononion subgranosum* (Egger), *Elphidium complanatum* (d'Orbigny), *E. depressulum* Cushman and *E. macellum* (Fichtel and Moll) (Figure 6).

Foraminiferal assemblage found in the range of 22.00–26.00 m consist of *Reussella spinulosa* (Reuss), *Haynesina germanica* (Ehrenberg), *Nonionella turgida* (Williamson), *Textularia bocki* Höglund, *T. truncata* Höglund, *Adelosina* cf. *cliarensis* (Heron-Allen and Earland), *A. duthiersi* Schlumberger, *A. mediterranensis* (Le Calvez), *A. carinata-striata* Wiesner, *A. pulchella* d'Orbigny, *Quinqueloculina seminula* (Linnaeus), *Quinqueloculina* cf. *vienensis* Le Calvez, *Pseudotriloculina* cf. *rotunda* (d'Orbigny), *Pseudotriloculina* sp., *Pyrgo elongata* (d'Orbigny), *Triloculina marioni* Schlumberger, *Triloculina* cf. *adriatica* Le Calvez, *T. asymmetrica* Said, *Lagena striata* (d'Orbigny), *Globigerinita glutinata* (Egger), *Globigerinoides ruber* (d'Orbigny), *Globigerinoides* sp., *Brizalina spathulata* (Williamson), *Fursenkoina acuta* (d'Orbigny), *Valvulineria bradyana* (Fornasini), *Eponides repandus* Fichtel and Moll, *Vonkleinsmidoides* sp., *Neoeponides* cf. *bradyi* (Le Calvez), *Rosalina bradyi* Cushman, *Hyalinea baltica* (Schröter), *Lobatula lobatula* (Walker and Jacob), *Planorbulina mediterranensis* d'Orbigny, *Aubignyna perlucida* (Heron-Allen and Earland), *Ammonia beccarii* (Linnaeus), *A. parkinsoniana* (d'Orbigny), *A. tepida* (Cushman), *A. compacta* (Hofler), *Challengerella bradyi* Billman, Hottinger and Oesterle, *Cribroelphidium poeyanum* (d'Orbigny), *Elphidium complanatum* (d'Orbigny), *E. crispum* (Linnaeus), *E. depressulum* Cushman (Figures 6, 10, 11).

Foraminifers observed in 28.00–31.00 m interval are *Textularia bocki* Höglund, *T. truncata* Höglund, *Adelosina mediterranensis* (Le Calvez and Le Calvez), *Adelosina partschi* (d'Orbigny), *A. pulchella* d'Orbigny, *Spiroloculina* cf. *angulosa* Cushman, *S. excavata* d'Orbigny, *Lachlanella andulata* (d'Orbigny), *Quinqueloculina* cf. *vienensis* Le Calvez and Le Calvez, *Quinqueloculina* sp., *Pseudotriloculina oblonga* (Montagu), *Triloculina marioni* Schlumberger, *T.* cf. *adriatica* Le Calvez and Le Calvez, *Triloculina trigonula* (Lamarck), *Bulimina marginata* d'Orbigny, *Reussella spinulosa* (Reuss), *Valvulineria bradyana* (Fornasini), *Eponides repandus* Fichtel and Moll, *Neoeponides* cf. *bradyi* (Le Calvez), *Lobatula lobatula* (Walker and Jacob), *Planorbulina mediterranensis* d'Orbigny, *Haynesina germanica* (Ehrenberg), *Nonionella turgida* (Williamson), *Ammonia beccarii* (Linnaeus), *A. parkinsoniana* (d'Orbigny), *A. compacta* (Hofler), *Challengerella bradyi* Billman, Hottinger and Oesterle, *Porosononion subgranosum* (Egger), *Elphidium crispum* (Linnaeus), *E. complanatum* (d'Orbigny) (Figures 6, 10, 11).

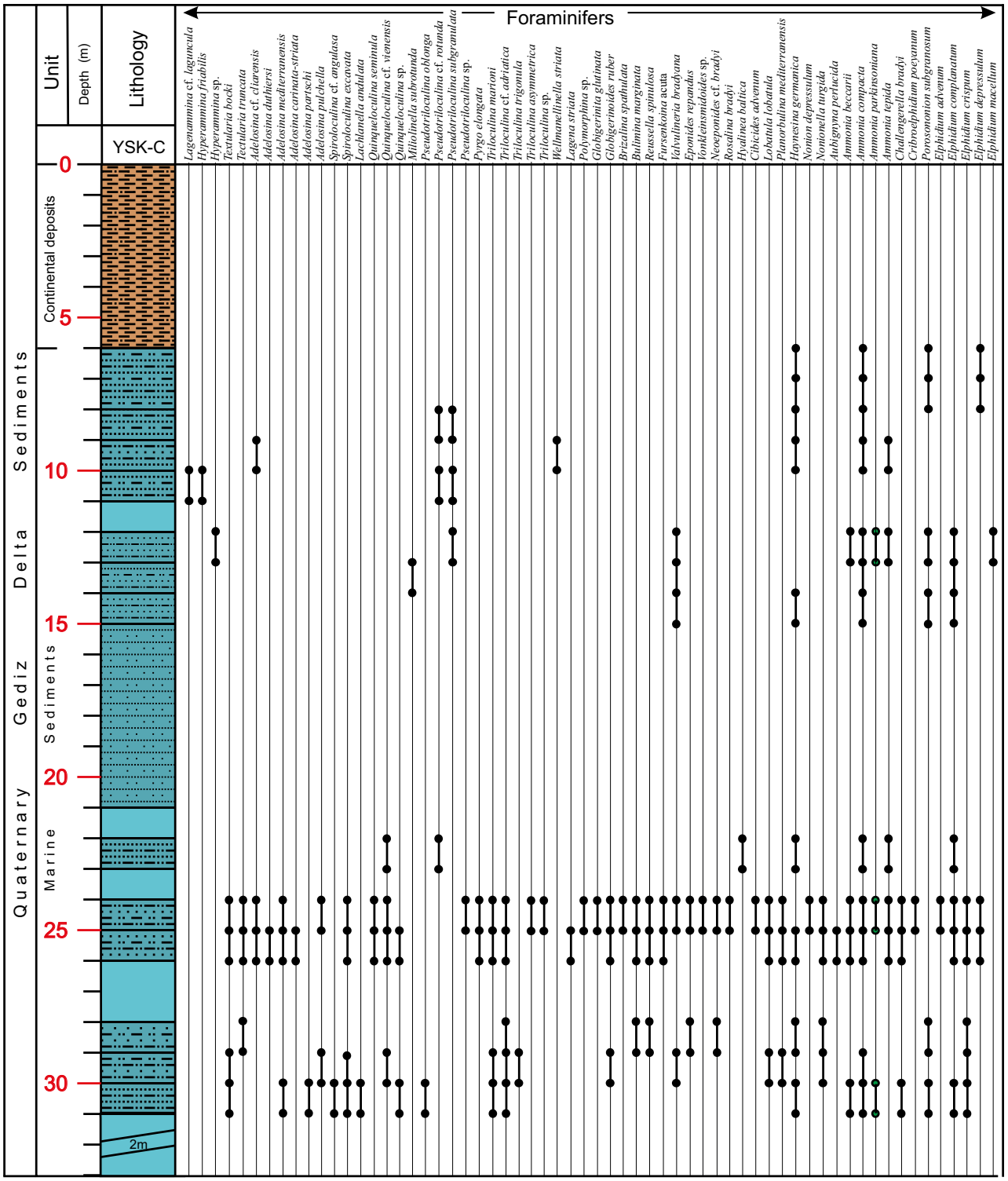


Figure 6. Vertical distribution of foraminifers in YSK-C core.

Considering the vertical distribution of the foraminifers described above, it is seen that there are 23 genera and 31 species in the range of 31.00–24.00 m and 27 genera and 42 species in the range of 24.00–22.00 (Figure 6). Towards the top, there is a drastic decrease in the number of genera and species at the 15.00–06.00 m ranges (11

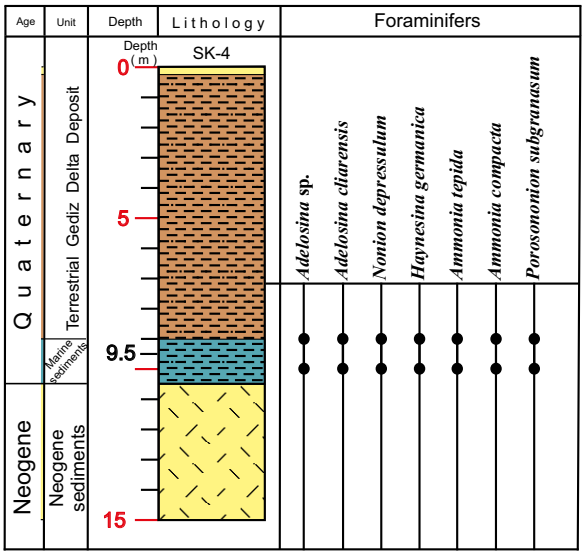


Figure 7. Vertical distribution of foraminifers in SK-4 core.

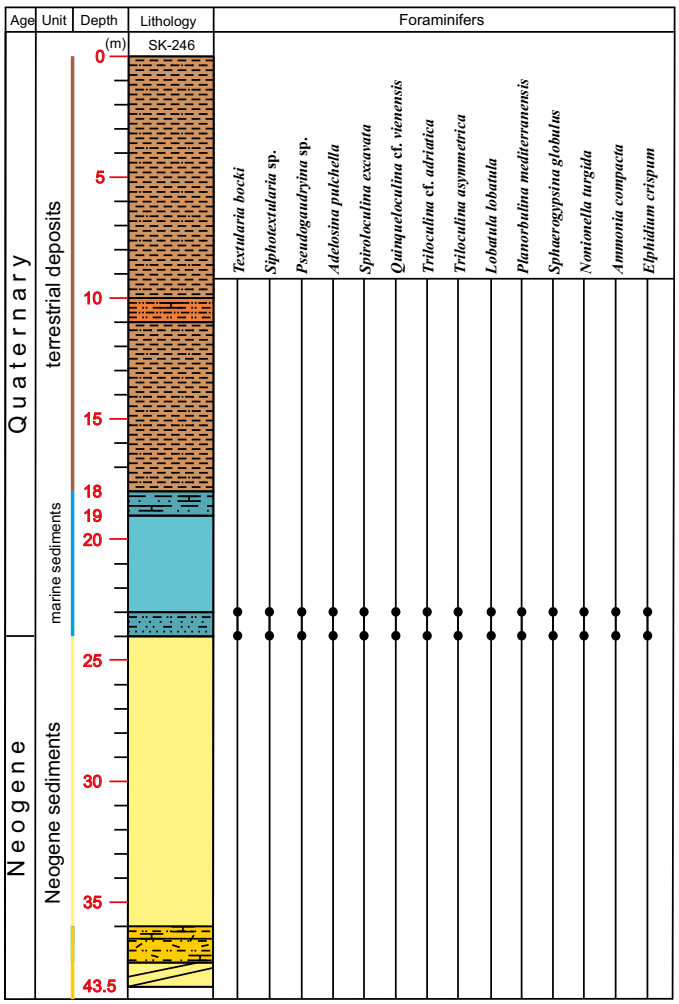


Figure 8. Vertical distribution of foraminifers in SK-246 core.

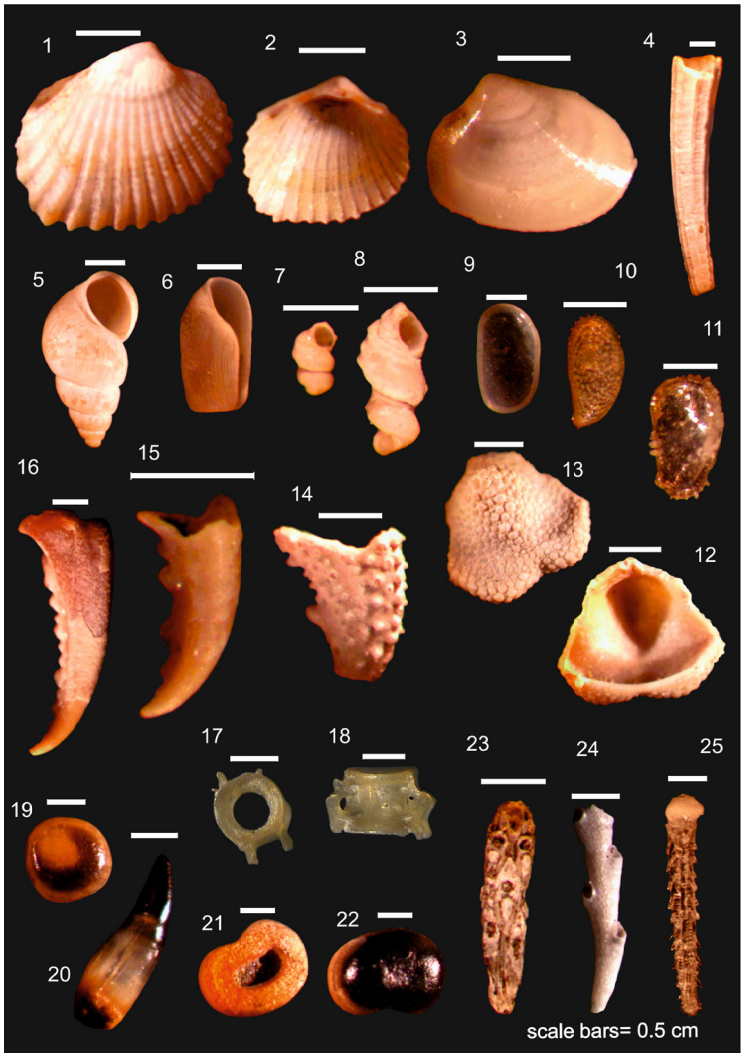


Figure 9. 1) Gastropod. External view; x 25; YSK-C, 10.00–11.00 m, 2) Bivalve. External view; x 25; YSK-C 24.00–25.00 m, 3) Gastropod. External view; x 25; YSK-C 24.00–25.00 m, 4) Gastropod. External view; x 25; YSK-C 9.00–10.00 m, 5–6) Gastropod. External view; x 25; YSK-C 24.00–25.00 m, 7) Gastropod. External view; x 25; YSK-C 10.00–11.00 m, 8–9) Echinoid fragments. External view; x 32; YSK-C 10.00–11.00 m, 10–11) Ostracod. External view; x 32; YSK-C 24.00–25.00 m, 12) Ostracod. External view; x 32; YSK-C 13.00–14.00 m, 13) Decapod fragment. External view; x 25; YSK-C 8.00–9.00 m, 14) Decapod fragment. External view; x 25; YSK-C 24.00–25.00 m, 15) Sponge spicules External view; x 40; YSK-C 23.00–24.00 m, 16) Sponge spicules External view; x 40; YSK-C 28.00–29.00 m, 17) Bryozoa fragment External view; x 25; YSK-C 24.00–25.00 m, 18) Bryozoa fragment. External view; x 32; YSK-C 25.00–26.00 m, 19) Fish vertebrae fragments; x 32; YSK-C 24.00–25.00 m, 20) Fish vertebrae fragments; x 32; YSK-C 24.00–25.00 m, 21–23) Fish tooth. External view; x 32; YSK-C 10.00–11.00 m.

genera, 16 species). Two planktonic foraminifera species, *Globigerinita glutinata* (Egger) and *Globigerinoides ruber* (d'Orbigny) species are also seen in the same range (Figures 6, 10).

4.2.3. Fossil content of the SK-4 core

The marine beds of SK-4 core are abundant in bivalves, gastropods, ostracod fragments, and foraminifers. The foraminifer assemblage consists of 7 species belonging to 5 genera (Figure 7). *Ammonia compacta* (Hofler) and *Haynesina germanica* (Ehrenberg) are common in this group. while *Adelosina* sp., *Nonion depressulum* (Walker and Jacob), *Ammonia tepida* (Cushman), *Porosononion subgranasum* (Egger) are found less, *Adelosina cliarensis* (Heron-Allen and Earland) is rare (Figures 7, 10, 11). These foraminifera of the SK-4 core are also found in the YSK-C core.

4.2.4. Fossil content of SK-246 core

The SK-246 drilling, located near a Neogene-aged outcrop at the E-NE boundary of the Gediz Delta at the western edge of the Menemen district was carried out on recent

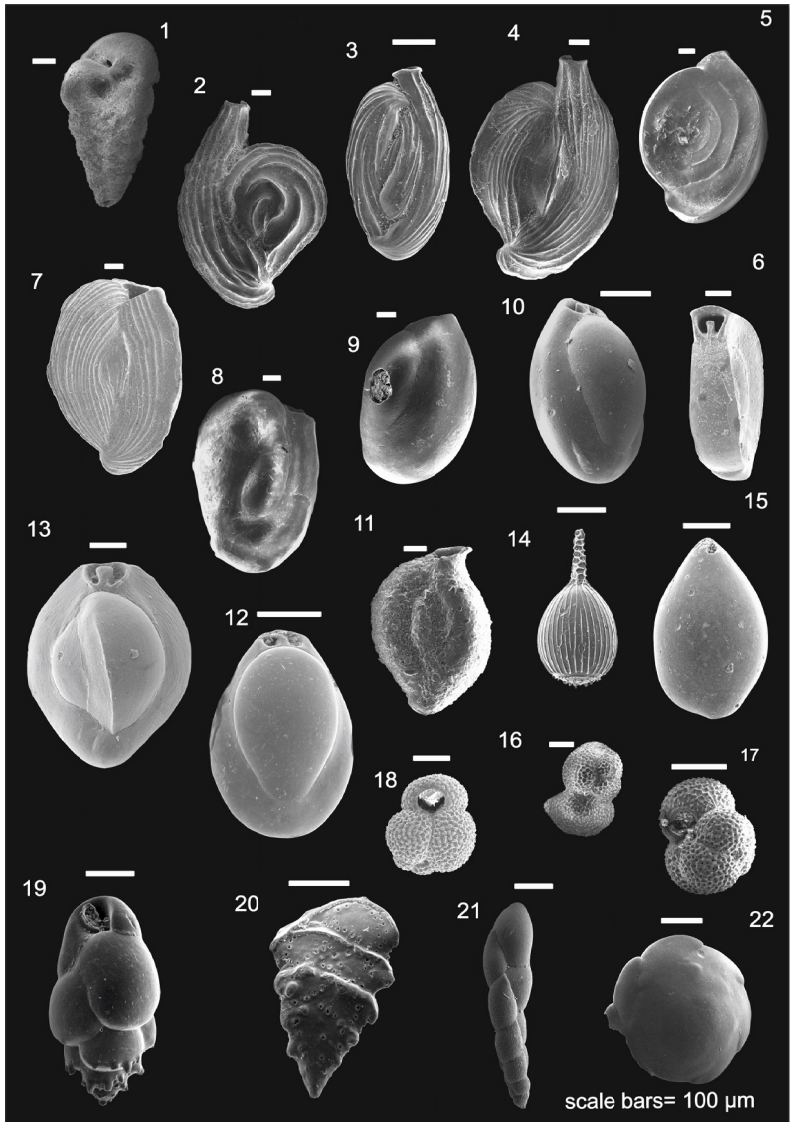


Figure 10. Images of benthic and planktonic foraminifers identified in this study. 1) *Textularia bocki* Hoglund. External view; YSK-C 25.00–26.00 m, 2) *Adelosina mediterranensis* (Le Calvez, J. and Y.). External view; YSK-C 30.00–31.00 m, 3) *Adelosina carinata-striata* Wiesner. External view; SK-4 9.50 m 4) *Adelosina partschi* (d'Orbigny). External view; YSK-C 29.00–30.00 m 5–6) *Spiroloculina excavata* d'Orbigny. External view and apertural view; YSK-C 29.00–30.00 m, 7) *Lachlanella undulata* (d'Orbigny). External view; YSK-C 30.00–31.00 m, 8) *Pseudotriloculina oblonga* (Montagu). External view; YSK-C 30.00–31.00 m 9–10) *Pseudotriloculina* cf. *rotunda* (d'Orbigny). External view; YSK-C 30.00–31.00 m 11) *Pseudotriloculina subgranulata* (Cushman). External view; YSK-C 10.00–11.00 cm 12) *Pyrgo elongata* (d'Orbigny). External view; YSK-C 24.00–25.00 m 13) *Triloculina marioni* Schlumberger. External view; YSK-C 10.00–11.00 m, 14) *Lagena striata* (d'Orbigny). External view; YSK-C 24.00–25.00 m 15) *Polymorphina s*p. External view; YSK-C 24.00–25.00 m 16) *Globigerinita glutinata* (d'Orbigny). External view; YSK-C 25.00–26.00 m, 17) *Globigerinoides ruber* (d'Orbigny). External view; YSK-C 24.00–25.00 m, 18) *Globigerinoides ruber* (d'Orbigny). External view; YSK-C 25.00–26.00 m, 19) *Bulimina marginata* d'Orbigny. External view; YSK-C 25.00–26.00 m, 20) *Reusella spinulosa* (Reuss). External view; YSK-C 24.00–25.00 m 21) *Fursenkoina acuta* (d'Orbigny). External view; YSK-C 25.00–26.00 m 22) *Neoeponides bradyi* (La Calvez). External view; spiral side, YSK-C 7.00–8.00 m.

alluvion (Figure 2). In this drilling, fossiliferous layers were observed in 37.50–36.00 m, 24.00–23.00 m, and 19.00–18.00 m intervals, 1–2 mm in size bivalves, gastropods, bryozoa fragments and foraminifers were detected only in 24.00–23.00 m interval. In the ranges of 37.50–36.00 m and 19.00–18.00 m, poorly preserved and fragmented sand-sized gastropods and probable bivalvia and ostracod fragments were observed. The foraminifer assemblage of the 24.00–23.00 m interval consists of 13 genera and 14 species (Figures 8, 10, 11). *Ammonia compacta* (Hofler)

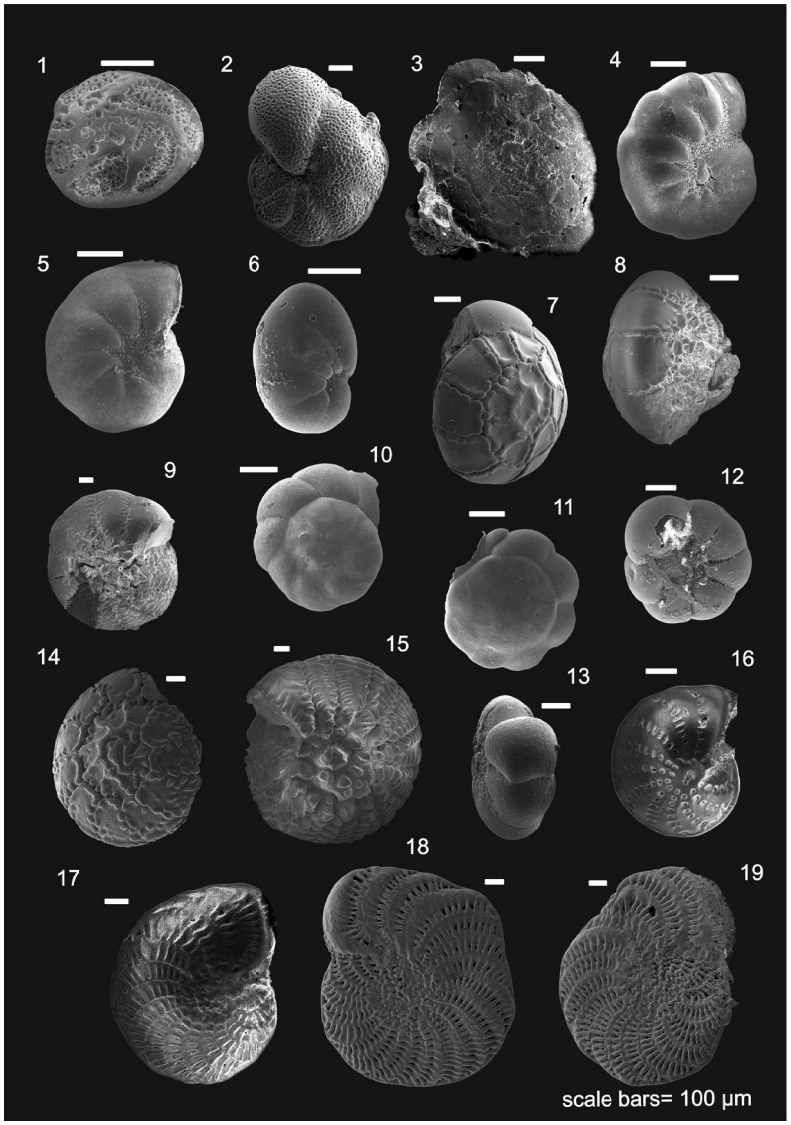


Figure 11. Images of benthic foraminifers identified in this study. 1) *Rosalina bradyi* Cushman. External view; spiral side, YSK-C 24.00–25.00 m 2) *Lobatula lobatula* (Walker and Jacob). External view; spiral side, YSK-C 24.00–25.00 m 3) *Planorbulina mediterranensis* d'Orbigny. External view; YSK-C 29.00–30.00 m 4) *Haynesina germanica* (Ehrenberg). External view; YSK-C 9.00–10.00 m 5) *Nonion depressulum* (Walker&Jacoob) External view; YSK-C 25.00–26.00 m 6) *Nonionella turgida* (Williamson). External view; spiral side, YSK-C 25.00–26.00 m 7) *Ammonia compacta* (Hofler). External view; spiral side, YSK-C 24.00–25.00 m, 8) *Ammonia compacta* (Hofler). External view; umbilical side, SK-246 23.00–24.00 m, 9) *Ammonia compacta* (Hofler). External view; umbilical side SK-246 23.00–24.00 m, 10) *Ammonia compacta* Cushman. External view; spiral side, YSK-C 24.00–25.00 m, 11) *Ammonia tepida* Cushman. External view; spiral side, SK- 4 9.00–10.50 m, 12) *Ammonia tepida* Cushman. External view; umbilical side, YSK-C 9.00–10.00 m, 13) *Ammonia tepida* Cushman. External view, YSK-C 9.00–10.00 m, 14) *Challengeralla bradyi* Billman, Hottinger and Oesterle. External view; spiral side, YSK-C 24.00–25.00 m, 15) *Challengeralla bradyi* Billman, Hottinger and Oesterle. External view; umbilical side, YSK-C 30.00–31.00 m, 16) *Elphidium advenum* (Cushman). External view, YSK-C 9.00–10.00 m, 17) *Elphidium complanatum* (d'Orbigny). External view; YSK-C 8.00–9.00 m, 18) *Elphidium complanatum* (d'Orbigny). External view; YSK-C 10.00–11.00 m, 19) *Elphidium complanatum* (d'Orbigny). External view; YSK-C 8.00–9.00 m.

and *Elphidium crispum* (Linnaeus) species are relatively common in this community. On the other hand, *Textularia bocki* Hoglund, *Adelosina pulchella* d'Orbigny, *Spiroloculina excavata* d'Orbigny, *Quinqueloculina* cf. *viennensis* Le Calvez and Le Calvez, *Lobatula lobatula* (Walker and Jacob), *Planorbulina mediterranensis* d'Orbigny and *Nonionella turgida* (Williamson) individuals are not common. *Siphotextularia* sp., *Pseudogaudryina* sp., and

Sphaerogypsina globulus (Reuss) individuals were found only at this core, not in the YSK-C and SK-4 cores.

5. ESR age of the YSK-C core

The ESR technique was used to date the gastropod and bivalve shells compiled from the marine layers at 9.00–8.00 m, 25.00–24.00 m, 26.00–25.00 m intervals of the YSK-C core. Conducted studies have shown that ESR ages of marine gastropod and bivalve shells belong to the Latest Pleistocene-Early Holocene times (Aydın, 2015). The obtained linear uranium uptake (LU) ages are more consistent with the geological expectation of the environment. Preferring LU (Linear up take) instead of EU (early up take) is a choice based on the ^{238}U, ^{232}Th, ^{40}K amounts obtained from the analysis (ICP-MS) of the sedimentary sample taken from the surrounding of the sample, geological dose value, sample thickness, moisture content of the sample and sediments.

ESR analysis graphs of selected samples of the YSK-C core were drawn for the calculations (Figures 5a, 5b). These calculations were made on dose-response curves, and the g = 2.0016 signal of the shell sample taken at 26.00–25.00 m, the g = 2.0018 signal of the shell sample taken at 25.00–24.00 m, and the g = 2.0012 signal of the shell sample taken at 9.00–8.00 m were used. Accordingly, the YSK-C core yields an age of 19.9 ± 2.2 ka for the interval between 26.00 and 25.00 m, 15.3 ± 2.0 ka for the interval between 25.00 and 24.00 m, and 11.4 ± 1.5 ka for the interval between 9.00 and 8.00 m (Figure 12). Consequently, the uppermost 6 m-thick continental deposit layer, the top of which corresponds to the modern-day depositional phase is younger than 11.4 ka.

6. Discussion

Considering the presence of Neogene aged volcanic rocks around and at the basement of the Delta, it can be inferred that the volcanic pebbles encountered in the YSK-C core were derived from the Neogene basement. However, mica sands must be derived from the Menderes Massif, which is far from the Delta and contains mica schists. The SK-246 core contains a definite marine level with abundant foraminifers between 24.00–23.00 m and a probable marine level with molluscs and ostracod fragments between 19.00 and 18.00 m. This 24.00–18.00 m interval

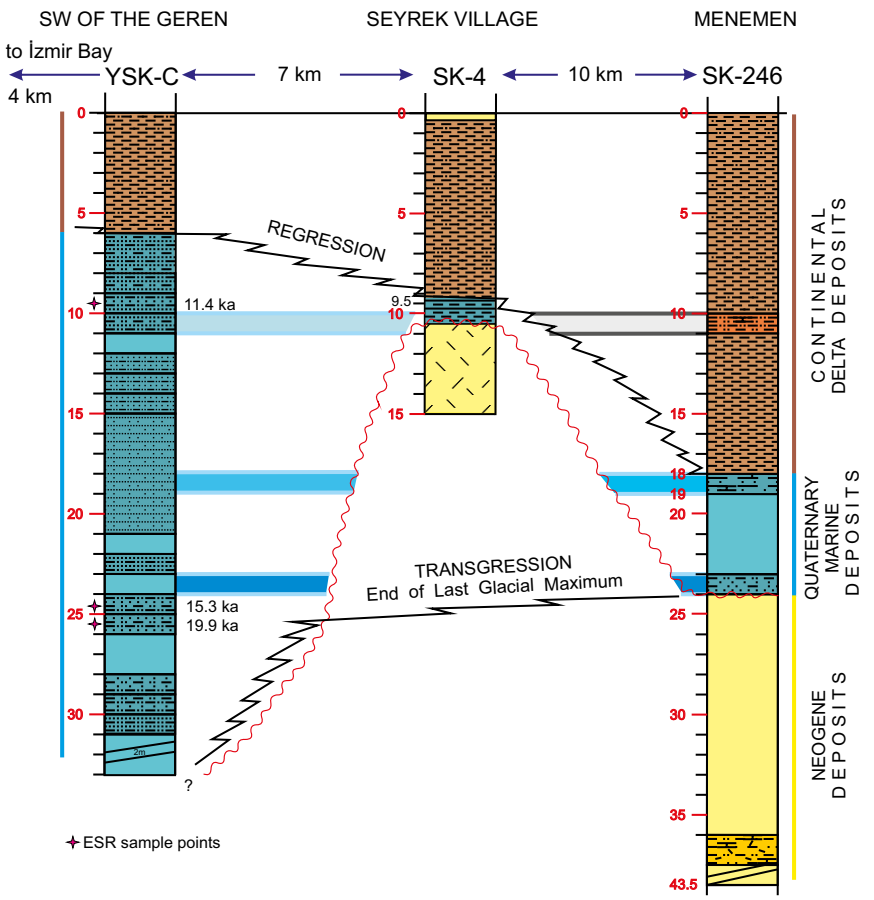


Figure 12. Lithostratigraphic, biostratigraphic and environmental correlations of YSK-C, SK-246, and SK-4 cores.

can be interpreted maximum transgression level after the LGM. In the 19.00–18.00 m interval of SK-246 core, marine fauna is absent except for some fragments. For this reason, this level has been considered as "probable marine". However, it is clear that the post-LGM transgression had reached the edge of Menemen town in the range of 24.00–23.00 m due to the abundant marine fauna (Figures 8, 12, 13).

The significant decrease in the thickness of the marine layers from the YSK-C (> 29 m) to SK-246 (maximum 7.00 m) is the result of the west-to-east progression of the post-LGM transgression over the Neogene basement (Figures 12, 13), where YSK-C site represents the deeper and SK-246 site represents the shallower parts of the marine environment. Similarly, the thinning of the terrestrial sediment layers from the SK-246 core to the SK-4 and YSK-C cores (18.00 m, 9.00 m, and 6.00 m, respectively) reflects the last coastal retreat from east to West (Figure 12).

A few (5 individuals) planktic foraminifers belonging to *Globigerinita glutinata* (Egger), *Globigerinoides ruber* (d'Orbigny) observed in the lower part of the YSK-C core may have been carried into the bay by sea movements or artificial means (Figure 6). Although their presence might relate to the deepening during the first period of sea progression following the LGM, there is no data indicating pelagic conditions. Therefore, their presence can be attributed to coincidental causes.

Based on the ESR ages obtained, the uppermost 6.00 m of continental deposit part of the YSK-C core must be younger than 11.4 ka. In this case, continental deposits of the delta are older than the previous age suggestions, which are 3 ka as suggested by Aksu and Piper (1983 and 1984), and 7 ka as predicted by Hakyemez et al. (2013).

The YSK-C core was terminated in the marine deposits of the delta at 35.00 m and accordingly, it can be considered that the marine sediments of the core are thicker than 35.00 m. This fact indicates that the marine stage of the delta should be older than 19.9 ka. Therefore, it is possible to infer that the Gediz Delta transgression started earlier than 20 ka or during the LGM, and the Aegean Sea coastline was further east of the YSK-C location, not in front of Foça contrary to the statement of Aksu and Piper (1983 and 1984). If the Aegean Sea

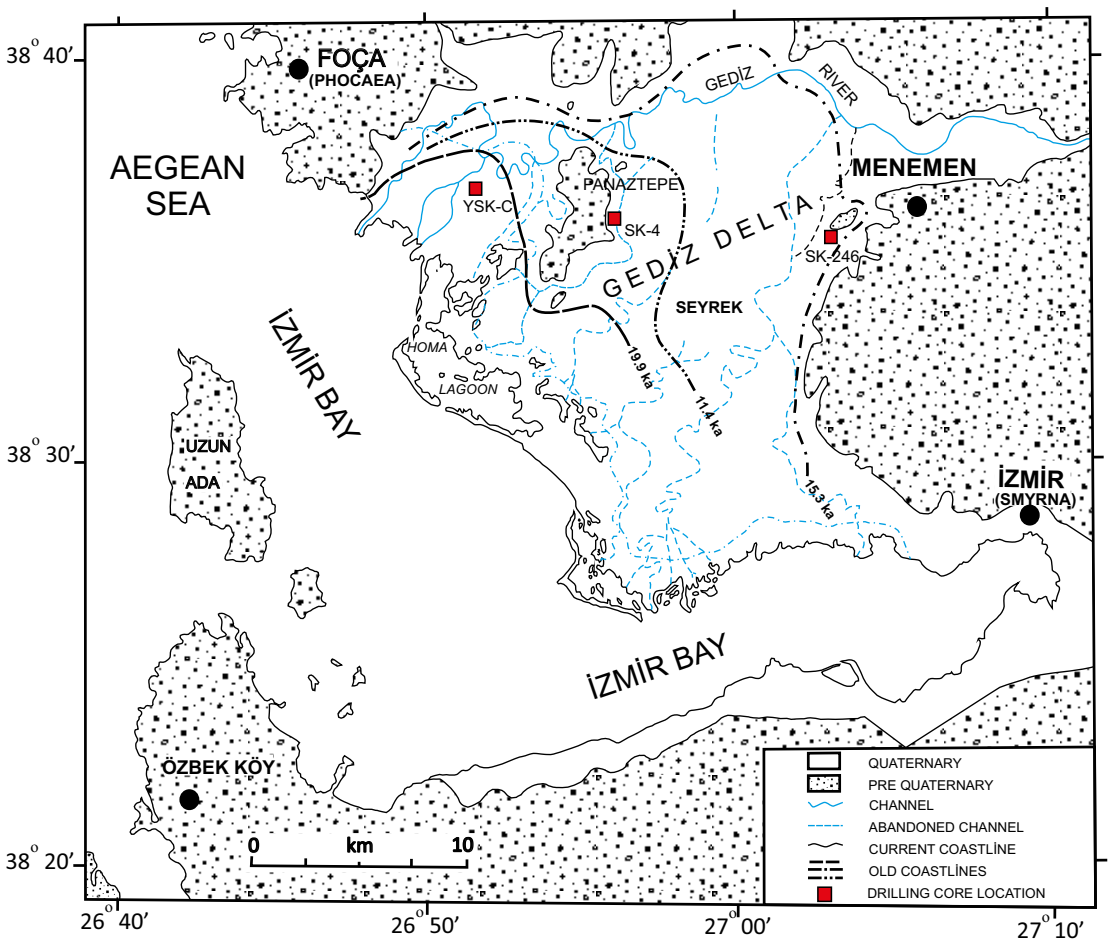


Figure 13. The inferred paleo coastline map of the Gediz Delta in the last 20 ka (Modified from Aksu and Piper, 1983).

coastline was located east of the YSK-C locality during the LGM, the marine level dated 15.3 ka between 24.00–23.00 m in the YSK-C core may mark the end of the LGM and onset of transgression. Thus, the marine level in the range of 24.00–23.00 m in the SK-246 core may correspond to the end of the LGM and indicate that the coastline reached Menemen (Figures 12, 13). While the available ESR and micropaleontological data combined with stratigraphical correlation allow us to make these interpretations, however, further ESR assessment of the marine sediments of the SK-246 and SK-4 cores is needed to verify the eustatic sea-level change and hence the paleo-shoreline for the time intervals identified in this study.

The rapid onset of the regression after the marine layers represented by the 24.00–18.00 m range in the SK-246 core supports that this level points to the end of the LGM transgression. Because, at this time, with the melting of the glaciers and-or snow cover of mountains in West Anatolia (Akçar et al., 2014; Sarıkaya and Ciner, 2015), the Gediz Graben Lake (Hakyemez et al., 2013) flowed westward via Emiralem Strait that caused the water and terrestrial sediments reach to the Gediz Delta in a short time and regression to begin. The presence of marine layers in the SK-246 core at 24.00–18.00 m indicates that the sea level rapidly increased from the west (YSK-C) to the east (SK-246).

In SKS-246 core, near Menemen, terrestrial beds are found 18 m in thickness. However, in the vicinity of Seyrek village, in the SK-4 core, this thickness is 8 m. Westward, near Geren, in the YSK-C core, 11 ka aged terrestrial beds are only 6 m in thickness (Figures 12, 13). This distribution pattern of the terrestrial clastics reflects that the terrestrial sediments of the Gediz River reached the YSK-C locality later than 11 ka and that the regression initiated very quickly in a few thousand years. These observations are not parallel to the findings of Hakyemez et al. (2013), who declared that the Gediz River started to flow to İzmir Bay at around 7 ka BP. This finding is also not coherent with the findings of Aksu and Piper (1998), who reported the Gediz River began to fill up the delta at around 3 ka BP.

Uzel et al. (2008, 2012) stated that the current Gediz Delta area is a part of the youngest Plio-Quaternary tectonosedimentary basin covering İzmir Bay. According to these authors, this half-graben basin developed under the control of tectonic events. However, the Gediz Delta area, which is the subject of this study, is located on the stable edge of the half-graben. Considering the morphology of the delta area, the horizontal geometry of marine layers, and their lateral continuity, there is not enough evidence of a tectonic impact causing the progradation and retrogradation of the delta shoreline, in the last 20 ka. For this reason, it is more appropriate to explain the evolution of the Gediz Delta, mostly with post-LGM eustatic sea-level change events over the last 20 ka. On the other hand, LGM-related studies in the region are scarce and tectonic assessment of the Gediz Delta region located within the İzmir-Balıkesir Transfer Zone (IBTZ) (Uzel and Sözbilir ,2008), Sözbilir et al. (2011), Uzel et al. (2012, 2013), and Özkaymak et al. (2013) have shown differences than that of the further east (Westaway, 2004, Maddy et al, 2016). Thus, it is not possible to explain a sudden transgression and regression with regional uplift/subsidence occurring in a very short time period of 15–20 ka. Similarly, Ocakoğlu (2020) reached results showing that in the last 400 ka of continental Quaternary sediments of Karacasu Graben (Aydın) located east of IBTZ, deposition was effective until the end of LGM and erosion was dominant from the end of LGM. The author argued that erosion was caused by the tectonic uplift governed by the high-angle margin faults of the Büyük Menderes Graben, but stated that high erosion rates occurred after the LGM. This is important as it reflects the effect of glacial and snow cover melting in Western Anatolia after the LGM, as in the Gediz Delta.

The YSK-C core containing abundant mica grains (derived from the Menderes Massif) in the range of 31.00–30.00 m indicates that during the deposition of this mica-rich level, the Gediz River was connected through a pass to the Gediz Graben and the mica-bearing sediments of the Gediz Graben Lake were flowing into the Gediz Delta (Figure 1).

When the YSK-C and SK-246 drilling cores are correlated, it is observed that even though the W-SW part of the Gediz Delta was continuously marine in facies from 19.9 ka to 11.4 ka ago, the E-NW part (around Menemen) was a marine environment only about 15 ka ago (Figures 12, 13).

On the other hand, in the YSK-C core, the increase in the number of genera and species from 22 m downwards, may suggest that the most ideal marine environment for foraminifers occurs between 31.00–22.00 m depending on the sea progress (Figures 6, 12). However, the decrease in the number of genera and species from 22 m upwards may reflect that the living conditions for benthic foraminifers changed due to the regression of the sea (Figures 6, 12). In the same way, at the top of the marine part of the sequence, in 10.00–6.00 m intervals, the relative dominance of genera *Ammonia* and other small-sized foraminifers can indicate that marine delta condition changes to a swamp-like environment (Caruso et al., 2011; Hohenegger, 2015; Louvari et al, 2019) (Figures 6, 12). When the foraminifer assemblages of all three boreholes are evaluated, in the Delta sequence the number of genera and species decreases from bottom to top and in the lateral direction (from YSK-C to SK-246). Nevertheless, the species belonging to SK-246 and SK-4 drillings are also found in YSK-C (Figures 6, 7, 8). In this case, a detailed environmental analysis cannot be

performed. On the other hand, similar benthic foraminifer fauna has been recorded in the Eastern Mediterranean region in environments ranging from infralittoral (0-50m) to lower epibathyal (400–500 m) environments (Aksu et al., 2002; Meric et al., 2004a, 2014) and some of them can also be encountered in estuarine environments (Ünsal et al., 2002; Irvalı and Çağatay, 2009). However, considering the morphology and geometry of the Gediz Delta, and given the identified foraminifers in the drill cores most abundant in the infralittoral environments and indicator species of circalittoral and epibathyal depths are absent, an infralittoral environment with a depth range of 0–50 m can be predicted for the Delta.

7. Conclusions

In this study, the Gediz Delta deposits were examined by using three drilling cores and adequate data on the vertical and lateral distributions of delta sediments were presented together with absolute ages obtained by applying the ESR method on marine shells for the time interval of the latest Pleistocene-Early Holocene for the first time. The marine layers of the western core dated by applying ESR were 19.9 ka (at 26.00–25.00 m), 15.3 ka (at 25.00–24.00 m), and 11.4 ka (at 9.00–8.00 m.) age, and these layers were stratigraphically correlated with the marine layers identified in the other two sediment cores. Sea-level changes were evaluated for this specific time interval through micropaleontological and sedimentological data achieved during this study. Our findings are as follows:

1. In the Gediz Delta, from west to east (up to the edge of the Menemen district), the latest Pleistocene-Holocene marine layers are represented by abundant marine fauna.

2. In the westernmost part of the delta, the marine layers of the YSK-C drilling core correspond to 19.9 ka, 15.3 ka, and 11.4 ka as obtained by applying ESR dating. Marine layers corresponding to 15.3 ka identified from the drilling YSK-C are stratigraphically correlated with marine layers of drilling core SK-246 located in the easternmost part. Therefore, drilling SK-246 represents the maximum transgression following the LGM.

3. Paleontological and ESR data evidence that 19.9 ka ago, the sea level was in the east of the YSK-C location and reached Menemen by 15.3 ka. Terrestrial sediments therefore must have started filling the Gediz Delta right after 15.3 ka and reached the westernmost part of the delta after a short time from 11.4 ka onwards.

Acknowledgements

Samples of this study were obtained within TÜBİTAK 106G159 KAMAG project drilling cores, supported by TÜBİTAK. We would like to thank DEU DAUM (Earthquake Research and Application Center) Directorate for allowing us to use the examples of this project. We would like to thank Mustafa Akgün and Gürkan Özden, the researchers of this project, for their special support. We also thank Radon Company and Murat Özgül for sharing detailed drilling information with us. This work is part of two MSc Thesis undertaken by Ekin Gökçe Benli and Hülya Aydın at the Institute of Natural and Applied Sciences in Dokuz Eylül University, İzmir, Turkey. We gratefully thank Doğan Yaşar, Bilal Sarı, and Erhan Akay (from Dokuz Eylül University) for their constructive discussions, and Ömer Feyzi Gürer and Şerafettin Çakır for their help during the laboratory work at Kocaeli University, Kocaeli, Turkey.

References

Akay E, Erdogan B (2001). Formation of subaqueous felsic domes and accompanying pyroclastic deposits on the Foça Peninsula İzmir, Turkey. International Geology Review 4: 661-674. https://doi.org/10.1080/00206810109465039

Akay E, Erdogan B (2004). Evolution of Neogene calc-alkaline to alkaline volcanism in the Aliağa-Foça region (Western Anatolia, Turkey). Journal of Asian Earth Sciences 24: 367–389. https://doi.org/10.1016/j.jseaes.2004.01.015

Akçar N, Yavuz V, Ivy-Ochs S, Yesilyurt S, Reber R et al. (2014). Extensive glaciations in Anatolian Mountains during the global Last Glacial Maximum. Geophysical Research Abstracts 16: EGU2014-4935. https://meetingorganizer.copernicus.org/EGU2014/EGU2014-4935.pdf

Akçığ Z, Pınar R, Türk N, Akgün M, Özden G et al. (2012). İzmir Metropol alanında kentsel dönüşüme taban oluşturacak zemin çalışmaları. Jeofizik Bülteni, pp. 76-79. https://www.jeofizik.org.tr/resimler/ekler/f7b937e4365cd00_ek.pdf?dergi=34 (in Turkish).

Aksu AE, Piper DJW (1983/1984). Progradation of the Late Quaternary Gediz Delta, Turkey. Marine Geology 54: 1-25. https://doi.org/10.1016/0025-3227(83)90006-3

Aksu AE, Hiscott RN, Kaminski MA, Mudie PJ, Gillespie H et al. (2002). Last glacial Holocene paleoceanography of the Black Sea and Marmara Sea: stable isotopic, foraminiferal and coccolith evidence. Marine Geology 190: 119-149. https://doi.org/10.1016/S0025-3227(02)00345-6

Aksu AE, Konuk T, Uluğ A, Duman M, Piper DJW (1990). Quaternary tectonic and sedimentary history of Eastern Aegean Sea Shelf area. Jeofizik 4: 3-35. https://dergipark.org.tr/tr/download/article-file/148949

Aksu AE, Yaşar D, Mudie, PJ, Gillespie H (1995). Late glacial Holocene paleoclimatic and paleoceanographic evolution of the Aegean Sea: micropaleontological and stable isotopic evidence. Marine Micropaleontology 25: 1-28. https://doi.org/10.1016/0377-8398(94)00026-J

Avşar N (2002). Gökçeada, Bozcaada ve Çanakkale üçgeni kıta sahanlığı (KD Ege Denizi) bentik foraminifer dağılımı ve taksonomisi. Yerbilimleri 23 (26): 53-75. https://dergipark.org.tr/tr/download/article-file/145522 (in Turkish).

Avşar N, Aksu A, Dinçer F (2006). Erdek Körfezi (GB Marmara Denizi) bentik foraminifer toplulukları. Yerbilimleri 27 (3): 125-141. https://dergipark.org.tr/tr/download/article-file/145588 (in Turkish).

Avşar N, Meriç E, Alramazanoğlu A, Dinçer F (2008). Antalya Körfezi (GB Türkiye) kıta sahanlığı bölgesi güncel bentik foraminifer toplulukları. Yerbilimleri 29 (3): 111-136. https://dergipark.org.tr/tr/download/article-file/145616 (in Turkish).

Avsar N, Meric E (2001). Çeşme-Ilıca Koyu (İzmir) termal bolgesi güncel bentik foraminiferlerinin sistematik dagılımı. Yerbilimleri 24: 13-22. https://dergipark.org.tr/tr/download/article-file/145500 (in Turkish).

Avsar N, Ergin M (2001). Spatial distribution of Holocene benthic foraminifera, Northeastern Aegean Sea. International Geology Review 8: 754-770. https://doi.org/10.1080/00206810109465046 (in Turkish).

Aydaş C, Engin B, Kapan S, Komut T, Aydın T et al. (2015). Dose estimation, kinetics and dating of fossil marine mollusc shells from northwestern part of Turkey. Applied Radiation and Isotopes 105: 72-79. https://doi.org/10.1016/j.apradiso.2015.07.053

Aydın H (2015). Gediz Deltası tortullarının (İzmir) elektron spin rezonans (ESR) tekniği ile tarihlendirilmesi. MSc, Dokuz Eylul University, İzmir (in Turkish).

Blackwell BAB, Skinner AR, Blickstein JIB, Montaya AC, Florentin J.A et al. (2016). ESR in the 21st century: from buried valleys and deserts to deep ocean and tectonic uplift. Earth-Sci Reviews 158: 125-159. https://doi.org/10.1016/j.earscirev.2016.01.001

Brennan BJ, Rink WJ, McGuirl, EL, Schwarcz, HP (1997). Beta doses in tooth enamel by "one-group" theory and the Rosy ESR dating software. Radiation Measurements 27 (2): 307-314. https://doi.org/10.1016/S1350-4487(96)00132-1

Brennan BJ, Rink, WJ, Rule EM, Schwarcz HP, Prestwich WV (1999). The ROSY ESR dating program. Ancient TL 17 (2): 45-53. http://ancienttl.org/ATL_17-2_1999/ATL_17-2_Brennan_p45-53.pdf

Çağatay MN, Görür N, Algan O, Eastoe C, Tchapalyga A et al. (2000). Late Glacial–Holocene palaeoceanography of the Sea of Marmara: timing of connections with the Mediterranean and the Black Seas. Marine Geology 167: 191–206. https://doi.org/10.1016/S0025-3227(00)00031-1

Caruso A, Cosentino C, Pierre C, Sulli A (2011). Sea-level changes during the last 41,000 years in the outer shelf of the southern Tyrrhenian Sea: Evidence from benthic foraminifera and seismostratigraphic analysis, Quaternary International, 232 (1): 122-131. https://doi.org/10.1016/j.quaint.2010.07.034

Cimerman F, Langer MR (1991). Mediterranean Foraminifera, Slovenska Akademija Znanosti in Umetnosti, Academia Scientiarum et Artium Slovenca, Ljubljana.

Clark PU, Shakun JD, Baker PA, Bartlein PJ, Brewer S et al., (2012). Global climate evolution during the last deglaciation. Proceedings Of The National Academy Of Sciences Of The United States Of America 109 (19): E1134-E1142. https://doi.org/10.1073/pnas.1116619109

Clark PU, Dyke AS, Shakun JD, Carlson AE, Clark J et al. (2009). The Last Glacial Maximum. Science 325 (5941): 710-714. https://doi.org/10.1126/science.1172873

Dias, JMA, Boski T, Rodrigues A and Magalhães F (2000). Coast line evolution in Portugal since the Last Glacial Maximum until present - a synthesis. Marine Geology 170 (1): 177–186. https://doi.org/10.1016/S0025-3227(00)00073-6

Dönmez M (1992). 1/25000 ölçekli sayısal jeoloji haritaları, Urla K17 C-3, C-4, İzmir K18 D-4 paftaları, Türkiye Jeoloji Veri Tabanı, Jeoloji Etüdleri Dairesi Başkanlığı, Maden Tetkik ve Arama Ggenel Müdürlüğü; Ankara, Turkey.

Emre T, Sözbilir H, Gökçen N (2006b). Neogene Quaternary stratigraphy of Kiraz-Beydağ region, Küçük Menderes Graben, West Anatolia. Mineral Research and Exploration of Turkey (MTA) Bulletin 132: 1–32. https://dergipark.org.tr/tr/download/article-file/44701

Engin B, Yesilyurt SK, Taner G, Demirtas H, Eken M (2006). ESR dating of Soma (Manisa, West Anatolia-Turkey) fosil gastropoda shells. Nuclear Instruments and Methods in Physics Research Section B: Beam Interactions with Materials and Atoms 243 (2): 397-406. https://doi.org/10.1016/j.nimb.2005.09.008

Erdoğan B (1990). İzmir–Ankara Zonu'nun İzmir ile Seferihisar arasındaki bölgede stratigrafik özellikleri ve tektonik evrimi. Bulletin of Turkish Association of Petroleum Geologists (TAPG) 2 (1): 1–20. http://tpjd.org.tr/images/bultenler/pdf/aralik1990.pdf (in Turkish).

Ergin Z, Kadir S, Keskin Ş, Turhan-Akyüz N, Yaşar D (2007). Late Quaternary climate and sea-level changes recorded in sediment composition off the Büyük Menderes River Delta (Eastern Aegean Sea, Turkey). Quaternary International 167–168: 162–176. https://doi.org/10.1016/j.quaint.2007.02.009

Evans AM, Flatman JC, Flemming NC (editors.) (2014). Prehistoric Archaeology on the Continental Shelf: A Global Review. New York: Springer.

Fairbanks RG, (1989). A 17,000-year glacio-eustatic sea level record: influence of glacial melting rates on the Younger Dryas event and deep-ocean circulation. Nature 342: 637-642. https://doi.org/10.1038/342637a0

Göktaş F, (2014). Karaburun Yarımadası kuzey kıyı kesiminin neojen stratigrafisi. Maden Tetkik Arama Dergisi (MTA) 148: 43-60. https://doi.org/10.19076/mta.77504 (in Turkish).

Grün R (1989). Electron spin resonance (ESR) dating. Quaternary International 1: 65-109. https://doi.org/10.1016/1040-6182(89)90010-4

Hakyemez HY, Erkal T, Göktas F (1999). Late Quaternary evolution of the Gediz and Büyük Menderes grabens Western Anatolia, Turkey. Quaternary Science Reviews 18 (4-5): 549-554. https://doi.org/10.1016/S0277-3791(98)00096-1

Hakyemez HY, Göktaş F, Erkal T (2013). Gediz Grabeninin Kuvaterner Jeolojisi ve evrimi. Türkiye Jeoloji Bülteni 56 (2): 1-26. https://dergipark.org.tr/tr/pub/tjb/issue/28126/298799 (in Turkish).

Helvacı C, Ersoy EY, Sözbilir H, Erkal F, Sümer Ö et al. (2009). Geochemistry and 40Ar/39Ar Geochronology of Miocene volcanic rocks from the Karaburun Peninsula: implications for amphibole-bearing lithospheric mantle source, Western Anatolia. Journal of Volcanology and Geothermal Research 185 (3): 181-202. https://doi.org/10.1016/j.jvolgeores.2009.05.016

Herodotus, with english translation by Godley AD (editor) (1920). Historiae I-IV: The Loeb Classical Library, 4 volumes in greek and english, London-New York.

Hohenegger J (2005). Estimation of environmental paleogradient values based on presence/absence data : a case study using benthic foraminifera for paleodepth estimation 217: 115–130. https://doi:10.1016/j.palaeo.2004.11.020

Hottinger L, Halicz E, Reiss Z (1993). Recent foraminiferida from the Gulf of Aqaba, Red Sea. Slovenica Akademija Znanosti in Umetnosti, Academia Scientiarum et Artium Slovenica: Ljublijana.

Ikeya M, Ohmura K (1981). Dating of Fossil Shells with Electron Spin Resonance: The Journal of Geology: https://doi.org/10.1086/628583

Ikeya M (1993). New Applications of Electron Epin Resonance, Dating Dosimetry and Microscopy: Osaka, Japan: World Scientific Publication. https://doi.org/10.1142/1854

Irvalı N, Çağatay M N (2009). Late Pleistocene–Holocene history of the Golden Horn Estuary, Istanbul. Geo-Marine Leters 29 (3): 151-160. https://10.1007/s00367-008-0129-z

İşintek İ, Altıner D, Özkan-Altıner S (2007). Foraminiferal and algal biostratigraphy and paleogeographic implications of the Mesozoic carbonate bodies between İzmir and Soma (Manisa). The Scientific And Technological Research Council Of Turkey (TÜBİTAK) report.

Kaminski MA, Aksu AE, Box M, Hiscott RN, Filipescu S et al. (2002). Late Glacial to Holocene benthic foraminifera in the Marmara Sea: implications for Black Sea-Mediterranean Sea connections following the last deglaciation. Marine Geology 190 (1-2): 165-202. https://doi.org/10.1016/S0025-3227(02)00347-X

Kaya O, Ünay E, Saraç G, Eichhorn S, Hassenrück S et al. (2004). Halitpaşa Transpressive Zone: Implications for an Early Pliocene compressional phase in central Western Anatolia, Turkey. Turkish Journal of Earth Sciences 13: 1-13. https://doi.org/10.3906/yer-0402-1

Kayan İ, Önder E (2016). Sedimantolojik ve Paleontolojik Verilerle Gediz Delta Ovasında (İzmir) alüvyal jeomorfoloji araştırmaları. Ege Coğrafya Dergisi 24 (2): 1-27. https://dergipark.org.tr/tr/download/article-file/234578 (in Turkish).

Kazancı N (2009). Neojen-Kuvaterner sınırının değişmesi ve beklenen gelişmeler. Türkiye Jeoloji Bülteni 52 (3), 367-374. https://dergipark.org.tr/tr/pub/tjb/issue/28365/301601 (in Turkish).

Küçükuysal C, Engin B, Türkmenoğlu AG, Aydaş C (2011). ESR dating of calcrete nodules from Bala, Ankara (Turkey): Preliminary results. Applied Radiation and Isotopes 69 (2): 492-499. https://doi.org/10.1016/j.apradiso.2010.10.005

Lambeck K, Esat TM, Potter EK (2002). Links between climate and sea levels for the past three millíon years. Nature 4l9 (6903): 199-206. http://dx.doi.org/10.1038/nature01089

Lambeck K, Purcell A (2005). Sea-level change in the Mediterranean Sea since the LGM: model predictions for tectonically stable areas. Quaternary Science Review 24 (18-19): 1969–1988. https://doi.org/10.1016/j.quascirev.2004.06.025

Lericolais G, Bulois C, Herve G, Guichard G (2008). High frequency sea level fluctuation recorded in the Black Sea since the LGM. Global and Planetary Chance 66 (1): 65-75. https:/doi.org./10.1016/j.gloplacha.2008.03.010

Li G, Li P, Liu Y, Qiao L, Ma Y, Xu J et al. (2014). Sedimentary system response to the global sea level change in the East China Seas since the last glacial maximum. Earth-Science Reviews 139: 390–405. https://doi.org/10.1016/j.earscirev.2014.09.007

Louvari MA, Drinia H, Kontakiotis G, Di Bella L, Antonarakou A et al. (2019). Impact of latest-glacial to Holocene sea-level oscillations on central Aegean shelf ecosystems: A benthic foraminiferal palaeoenvironmental assessment of South Evoikos Gulf, Greece. Journal of Marine Systems 199: 103-181. https://doi.org/10.1016/j.jmarsys.2019.05.007

Loeblich Jr AR., Tappan H (1988). Foraminiferal Genera and Their Classification. New York, ABD: Van Nostrand Reinhold Company.

Maddy D, Veldkamp A, Demir T, Gorp W van, Wijbrans JR et al. (2017). The Gediz River fluvial archive: A benchmark for Quaternary research in Western Anatolia. Quaternary Science Reviews 166: 289-306. https://doi.org/10.1016/j.quascirev.2016.07.031

Meric E, Avsar N (2001). Benthic foraminiferal fauna of Gokceada Island (Northern Aegean Sea) and its local variations. Acta Adriatica 42 (1): 125-150.

Meric E, Avşar N, Bergin F (2002). Midilli Adası (Yunanistan-kuzeydoğu Ege Denizi) bentik foraminifer faunası ve toplulukta gözlenen yerel değişimler. Çukurova University Journal of Geosound (40-41): 177-193 (in Turkish).

Meric E, Avsar N, Bergin F (2004a). Benthic foraminifera of Eastern Aegean Sea (Turkey) systematics and autoecology, Chambers of Geological Engineers of Turkey. İstanbul, Turkey: Turkish Marine Research Foundation.

Meriç E, Avsar N, Nazik A, Eryılmaz M, Yücesoy-Eryılmaz F, (2004b). Saros Körfezi'nin (Kuzey Ege Denizi) güncel bentik ve planktik foraminifer toplulukları ile çökel dağılımı. Çukurova University Journal of Geosound (44-45): 1-44 (in Turkish).

Meriç E, Avsar N., Nazik A, Alpar B, Yokeş B et al. (2005). Gemlik Körfezi yüzey çökellerinin foraminifer, ostrakod ve mollusk faunası, foraminifer kavkılarında gözlenen morfolojik amnomaliler ile sedimentolojik, hidrokimyasal ve biokimyasal özellikleri. Maden Tetkik ve Arama Dergisi (131): 21-48. https://doi.org/ 10.19076/MTA.3532 (in Turkish).

Meriç E, Avşar N, Yokeş MB, Dinçer F (2014). Atlas of recent benthic foraminifera from Turkey. Micropaleontology 60, 211–398. https://doi.org/ 10.47894/mpal.60.3.01

Mithen S (2004). After the ice: a global human history, 20.,000–5000 BC. Cambridge Massachusetts, United States: Harvard University Press.

Milker Y, Schmiedl G and Betzler C (2011). Paleobathymetric history of the Western Mediterranean Sea shelf during the latest glacial period and the Holocene: Quantitative reconstructions based on foraminiferal transfer functions. Palaeogeography Palaeoclimatology, Palaeoecology 307 (1), 324–338. https://doi.org/10.1016/j.palaeo.2011.05.031

Molodkov A (2020). The late pleistocene palaeoenvironmental evolution in northern Eurasia through the prism of the mollusc shell-based ESR dating evidence. Quaternary International 556: 180-197. https://doi.org/10.1016/j.quaint.2019.05.031

Murray J (2006). Ecology and Applications of Benthic Foraminifera, Cambridge University Press: Cambridge.

Ocakoğlu F (2020). Rapid Late Quaternary denudation of the Karacasu Graben in response to subsidence in the Büyük Menderes Corridor: Insights from morphotectonics and archaeogeology. Geomorphology 357. https://doi.org/10.1016/j.geomorph.2020.107107

Okay Aİ, Siyako M (1993). The new position of the İzmir-Ankara Neo Tethyan suture between İzmir and Balıkesir. in: Turgut, S., tectonics and hydrocarbon potential of Anadolia and surrounding regions. In: Proceedings of the Ozan Sungurlu Symposium; Ankara, Turkey. pp. 333-255. https://doi.org/10.3906/yer-0609-1

Okay AI and Altıner D (2007). A condensed Mesozoic succession north of İzmir: a fragment of the Anatolide-Tauride Platform in the Bornova Flysch Zone. Turkish Journal of Earth Sciences 16 (3): 257–279.

Özkaymak Ç, Sözbilir H, Uzel B (2013). Neogene–Quaternary evolution of the Manisa Basin: Evidence for variation in the stress pattern of the İzmir-Balıkesir Transfer Zone, western Anatolia. Journal of Geodynamics 65: 117-135. https://doi.org/10.1016/j.jog.2012.06.004

Plinius, with english translation by Rackham H (1967). Plinius Secundus C: Natural History volume V: LOEB Clasical Library, Harvard University Press, London.

Presidency of Turkey Republic, Precidency of state archives, (1984). Gediz Nehrinin Tahvil-i Mecrasının Değiştirilmesi Memlahalara Verdiği Zararın Önlenmesi, Ottoman archive, orginal document date: H21-07-1305 (Rumi calender), archive location number: 97-4104 (in Turkish).

Rink WJ (1997). Electron spin resonance (ESR) dating and ESR applications in quaternary science and archaeometry. Radiation Measurements 27 (5-6): 975-1025. https://doi.org/10.1016/S1350-4487(97)00219-9

Sarı B (2013). Late Maastrichtian-Late Palaeocene planktic foraminiferal biostratigraphy of the matrix of the Bornova Flysch Zone around Bornova (İzmir, Western Anatolia, Turkey). Turkish Journal of Earth Sciences 22 (1): 143-171. https://doi.org/10.3906/yer-1107-2

Seghedi I, Helvacı C, Pécskay Z (2015). Composite volcanoes in the south eastern part of İzmir–Balıkesir Transfer Zone, Western Anatolia, Turkey. Journal of Volcanology and Geothermal Research 291: 72–85. https://doi.org/10.1016/j.jvolgeores.2014.12.019

Sgarrella F, Moncharmont-Zei M (1993). Benthic foraminifera of the Gulf of Naples (Italy), systematic and autoecology. Bulletino della Societa Paleontologica Italiana 32 (2): 145-246.

Smith AD, Taymaz T, Oktay F, Yuce H, Alpar B et al. (1995). High-resolution seismic profiling in the Sea of Marmara (northwest Turkey): Late Quaternary sedimentation and sea-level changes. GSA Bulletin 107 (8): 923–936. https://doi.org/10.1130/0016-7606(1995)107<0923:HRSPIT>2.3.CO;2

Spratt T (1845). Observations on the Geology of the Southern Part of the Gulf of Smyrna and the Promontory of Karabournou. Quarterly Journal of the Geological Society 1: 156-162.

Skinner AR, Shawl CE (1994) ESR Dating of Terrestrial Quaternary Shells. Quaternary Science Reviews 13 (5): 679-684.

Sözbilir H, Sarı B, Uzel B, Sümer Ö, Akkiraz S (2011). Tectonic implications of transtensional supradetachment basin development in an extension-parallel transfer zone: the Kocaçay Basin, western Anatolia, Turkey. Basin Research 3 (4): 423-448. https://doi.org/10.1111/j.1365-2117.2010.00496.x

Stirling CH, Esat TM, Mcculloch MT, Lambeck K (1995). High-precision U-series dating of corals from Western Australia and implications for the timing and duration of the Last Interglacial. Earth and Planetary Science Letters 135 (1-4): 115-130. https://doi.org/10.1016/0012-821X(95)00152-3

Strabon, with an english translation by Jones HL (editor) (1917-1932). The Geography of Strabo I-VIII: The Loeb Classical Library, 8 volumes in greek and english, London, New York.

Strickland HF (1837). On the Geology of the Neighbourhood of Smyrna. Transactions of the Geological Society of London 1840, 2 (5): 393-402.

MTA (2002). Geological map of Turkey scale 1:500000, Şenel, M. (Ed.), General Directorate of Mineral Research and Exploration, Ankara, Turkey.

Tekin UK, Göncüoğlu MC (2007). Discovery of oldest (late Ladinian to middle Carnian) radiolarian assemblages from the Bornova Flysch Zone in western Turkey: Implications for the evolution of the Neotethyan Izmir-Ankara Ocean. Ofioliti 32 (2): 131-150. https://doi.org/10.4454/ofioliti.v32i2.353

Tekin UK, Göncüoğlu MC (2009). Late Middle Jurassic Late Bathonian-Early Callovian) Radiolarian Cherts from the Neotethyan Bornova Flysch Zone, Spil Mountains, Western Turkey, Stratigraphy and Geological Correlation 17 (3): 298-308. https://doi.org/10.1134/S086959380903006X

Tekin UK, Göncüoğlu MC, Uzuncimen S (2012). Radiolarian assemblages of Middle and Late Jurassic to early Late Cretaceous (Cenomanian) ages from an olistolith record pelagic deposition within the Bornova Flysch Zone in western Turkey. Société Géologique de France 183 (4): 307-318. https://doi.org/10.2113/gssgfbull.183.4.307

Türkecan A, Ercan T, Sevin D (1988). Karaburun Yarımadası'nın Neojen Volkanizması. General Directorate Mineral Research and Exploration Report no: 10185 (in Turkish).Ulusoy Ü, Anbar G, Bayarı S, Uysal T (2014). ESR and 230Th/234U dating of speleothems from Aladağlar mountain range (AMR) in Turkey. Quaternary Research 81: 367-380. https://doi.org/10.1016/j.yqres.2013.12.005

Uzel B, Sözbilir H (2008). A First record of strikeslip basin in western Anatolia and its tectonic implication: The Cumaovası basin as an example. Turkish Journal of Earth Sciences 7 (3). https://doi.org/10.3906/yer-0804-4

Uzel B, Sözbilir H, Özkaymak Ç (2012). Neotectonic Evolution of an Actively Growing Superimposed Basin in western Anatolia: The Inner Bay of İzmir, Turkey. Turkish Journal of Earth Science 21 (4): 439-471. https://doi.org/10.3906/yer-0910-11

Uzel B, Sözbilir H, Özkaymak Ç, Kaymakcı N, Langereis CG (2013). Structural evidence for strike-slip deformation in the Izmir-Balikesir transfer zone and consequences for late Cenozoic evolution of western Anatolia (Turkey). Journal of Geodynamics 65: 94-116. https://doi.org/10.1016/j.jog.2012.06.009

Ünsal İ, Rosso A, Meriç E, Avşar N, Çetin O (2002). Palaeoecology of Upper Pleistocene–Holocene bryozoan and foraminiferal assemblages from Kuşdili (Kadiköy, Istanbul, Turkey). Geobios 35: 735-743. https://doi.org/10.1016/S0016-6995(02)00085-2

Violante RA, Parker G (2004). The post-last glacial maximum transgression in the de la Plata River and adjacent inner continental shelf, Argentina. Quaternary International 114 (1): 167–181. https://doi.org/10.1016/S1040-6182(03)00036-3

Westaway R, Pringle M, Yurtmen S, Demir T, Bridgland D et al. (2004). Pliocene and Quaternary regional uplift in western Turkey: the Gediz River terrace staircase and the volcanism at Kula. Tectonophysics 391 (1-4): 121-169. https://doi.org/10.1016/j.tecto.2004.07.013

Yokoyama Y, Lambeck K, De Deckker P, Johnston P and Fifield LK (2000). Timing of the Last Glacial Maximum from observed sea-level minima. Nature 406: 713–716. https://doi.org/10.1038/35021035